Crosslinking of a CD4 Mimetic Miniprotein with HIV-1 Env gp140 Alters Kinetics and Specificities of Antibody Responses against HIV-1 Env in Macaques

Xiaoying Shen[a#], Willy M. Bogers[f], Nicole L. Yates [a], Guido Ferrari[a,e], Antu K. Dey[j,k], William T. Williams[a], Frederick H. Jaeger [a,], Kevin Wiehe[a], Sheetal Sawant[a], S. Munir Alam[a], Celia C. LaBranche[e], David C. Montefiori[a,e], Loic Martin[g], Indresh Srivastava[h], Jonathan Heeney[i,$] , Susan W. Barnett[j,l,$], Georgia D. Tomaras[a, b, c, d,e,#,$]

Running Head: CD4 Mimetic Alters HIV Env Antibody Response

[a]Duke Human Vaccine Institute, Departments of [b]Medicine, [c]Immunology, [d]Molecular Genetics and Microbiology, and [e]Surgery, Duke University Medical Center, Durham, NC, USA

[f] Biomedical Primate Research Centre, Rijswijk, The Netherlands

[g] Commissariat à l'Energie Atomique, iBiTecS, Service d'Ingénierie Moléculaire des Protéines, Gif-sur-Yvette F-91191, France

[h] Protein Sciences Corporation, Meriden, CT, USA

[i] Lab of Viral Zoonotics, Cambridge University, Cambridge, England

[j] Novartis Vaccines and Diagnostics, Inc., Cambridge, MA, USA

[k] Current address: International AIDS Vaccine Institute, New York, NY, USA

[l] Current address: Bill & Melinda Gates Foundation, Seattle, WA, USA

[#]Address correspondence to Drs. Xiaoying Shen, sxshen@duke.edu and Georgia D. Tomaras, gdt@duke.edu.

[$]These authors contributed equally.

Abstract

Evaluation of the epitope specificities, location (systemic, mucosal) and effector function of antibodies elicited by novel HIV-1 immunogens engineered to improve exposure of specific epitopes is critical for HIV-1 vaccine development. Utilizing an array of humoral assays, we evaluated the magnitude, epitope specificity, avidity and function of systemic and mucosal immune responses elicited by a vaccine regimen containing Env cross-linked to a CD4 mimetic miniprotein (gp140-M64U1) in rhesus macaques. Crosslinking of gp140 Env with M64U1 resulted in an earlier increase in both the magnitude and avidity of the IgG binding response compared to Env protein alone. Notably, binding IgG responses at an early time point correlated with Antibody Dependent Cellular Cytotoxicity (ADCC) function at the peak immunity time point, which was higher for the crosslinked Env group compared to the Env group alone. In addition, the crosslinked Env group developed higher IgG responses against a linear epitope in the C1 gp120 region of the HIV-1 envelope glycoprotein. These data demonstrate that structural modification of the HIV-1 envelope immunogen by crosslinking gp140 with the CD4 mimetic M64U1 elicited an earlier increase of binding antibody responses and altered the specificity of the IgG responses that correlated with the rise of subsequent antibody-mediated antiviral functions.

Importance

The development of an efficacious HIV-1 vaccine remains a global priority to prevent new cases of HIV-1 infection. Of the six HIV-1 efficacy trials to date, only one has demonstrated partial efficacy, and the immune correlates analysis of this trial revealed a role for binding antibodies and antibody Fc mediated effector functions. New HIV-1 envelope immunogens are being engineered to selectively expose the most vulnerable and conserved sites on the HIV-1 envelope with the goal of eliciting antiviral antibodies. Evaluation of the humoral responses elicited by these novel immunogen designs in nonhuman primates is critical for understanding

how to improve upon immunogen design to inform further testing in human clinical trials. Our results demonstrate that Env structural modifications that aim to mimic the CD4 bound conformation can result in earlier antibody elicitation, altered epitope specificity and increased antiviral function post immunization.

Introduction

A critical component in the path toward the development of a successful HIV-1 vaccine strategy is definition of the epitope specificities, location (systemic, mucosal) and effector function of antibodies elicited by novel HIV-1 immunogens engineered to improve exposure of specific epitopes. There is a growing body of evidence from animal models that antibodies can control virus replication (1-4) through elimination of infected cells (4), engagement of Fc-mediated antibody effector functions to limit founder viruses (2), and delay acquisition and/or prevent the establishment of infection (5-15) through mechanisms including virus neutralization (8-14, 16) and antibody Fc-mediated anti-viral functions (11, 15, 17). Together, these studies include both passive immunization strategies and vaccine approaches that have tested a range of antibody specificities, antibody isotypes and effector functions (broadly neutralizing, non-broadly neutralizing and antibody Fc-mediated antiviral activities), thus demonstrating that there is much diversity in the types of antibodies that may protect. However, there remains a gap in understanding how different immunogen designs specifically impact antibody specificities, kinetics and antiviral functions (*i.e.* neutralizing and non-broadly neutralizing).

There are numerous challenges for inducing broadly neutralizing antibody functions by vaccination, including but not limited to shielding of key epitopes by glycans, difficulty in presentation of the correct Env structures, and the unusual traits of broadly neutralizing antibodies (18, 19). In contrast, the one partially efficacious HIV-1 vaccine in humans demonstrated a potential role for non-broadly neutralizing antibodies in preventing HIV-1

acquisition (20). Non-broadly neutralizing antibodies include CD4-induced (CD4i) antibodies that target epitopes whose exposure is triggered by binding of HIV-1 Env gp120 to CD4 on the host cell. A recent study demonstrated that CD4i antibodies correlated with viremia control following mucosal challenge in rhesus macaques (3).

HIV vaccine strategies can involve modifying the structure of Env for improved exposure of CD4i epitopes. CD4i epitopes include co-receptor binding sites (21, 22) that are highly conserved (23-25) as well as variable loop domains (26, 27), some of which are easily elicited during natural HIV-1 infection (24, 28, 29). One immunogen design approach has utilized co-expression of CD4 in a single molecular structure with HIV-1 Env to promote binding and complex formation of CD4 and Env (3, 30-34). Another approach involves small molecule CD4 mimetic compounds, which have been shown to inhibit HIV-1 virus entry by competitively binding to CD4 binding site (CD4bs) (35, 36). A recent study further showed that CD4 mimetic compounds can activate or inactivate primary HIV Env trimers depending on properties of the CD4 mimetics and the Env trimer, and how many subunits of the trimer are bound (37). Several studies have explored biochemical cross-linking of synthetic CD4 mimetic molecules with Env proteins for improved CD4i epitope exposure (31, 38-41). In particular, a CD4-mimetic miniprotein M64U1, has been shown to expose both CD4i epitopes and co-receptor binding sites when covalently conjugated to Env gp140 (38), eliciting increased titers of CD4i antibody-mediated neutralization in rabbit immunization studies (38, 42). The gp140-M64U1 cross-linked vaccine was further tested in macaques (Bogers *et al*, submitted) and was shown to alter the kinetics of B cell responses and levels of neutralization and ADCC responses. Here we further characterized the magnitude, specificity, and kinetics of binding antibody responses and examined the correlation between these parameters of binding antibody response with that of antibody functions, providing novel evidence that the cross-linked gp140-M64U1 complex can

impact both the binding properties of and the antiviral functions mediated by Env-specific antibodies in primates.

MATERIALS AND METHODS

Animal study design.

Rhesus macaques of Chinese origin were housed at the Biomedical Primate Research Center (BPRC), The Netherlands. The study protocol and experimental procedures were approved by the institute's animal ethical care and use committee and were performed in accordance with Dutch law and International ethical and scientific standards and guidelines (Bogers *et al*, submitted). The study consisted of four groups of 6 animals each (**Table 1**). One group (gp140 group) received intramuscular immunization with 100 mg gp140 protein with the variable loop 2 (V2) deleted (SF162ΔV2 gp140), administered in adjuvant MF59; the second group (gp140-M64U1 group) received immunizations with 100 mg gp140 cross-linked with the CD4-mimetic M64U1 (gp140-M64U1, produced by incubating gp140 with M64U1-SH that contains an additional sulfhydryl group on the side chain of Lys4 at 1:3 gp140:M64U1-SH ratio) (38, 42), also in MF59. In addition, two control groups received either the M64U1/MF59 only (50 mg) or mock immunizations. All protein immunizations were delivered intramuscularly at week 0, 4, 24, 36, and 107 of study.

Binding antibody multiplex assay (BAMA).

Env-specific IgG and IgA responses in serum and in mucosal samples were measured as previously described (29, 43, 44). For quantification of IgA responses, IgG was depleted from sera using Protein G HP MultiTrap Filter Plates (GE Healthcare Life Sciences). Mucosal specimens were filtered, buffer-exchanged, and concentrated to equal volumes before measurement of total and specific antibody. The rectal wash samples were examined and none had visual blood contamination. Total IgG concentration in each mucosal sample was determined by macaque total IgG ELISA, and specific activity was calculated as: Specific

activity= (MFI x dilution)/total antibody. For characterization of CD4 binding site (CD4bs) and CD4-inducible (CD4i) antibodies, a CD4bs and CD4i differential binding antigen panel was used for BAMA, which includes the wildtype (WT) YU2 gp120 core, resurfaced stabilized core 3 (RSC3), HXB2 8b core, and their mutants containing mutations to amino acids that are known to be required for binding by CD4bs or CD4i antibodies (proteins kindly provided by Dr. Mascola, Vaccine Research Center). Relative levels of CD4bs and CD4i specificities were calculated as the MFI of WT: MFI of mutant ratios for samples that bound to both WT and mutant with MFI>100 and at least 3-fold over the MFI of matched baseline (wk0) samples.

Linear epitope mapping peptide microarray. Linear epitope mapping was performed as previously described (45, 46) with modifications. Briefly, array slides were provided by JPT Peptide Technologies GmbH (Berlin, Germany) by printing a peptide library designed by Dr. B. Korber (Los Alamos National Laboratory) onto Epoxy glass slides (PolyAn GmbH, Germany). The library contains overlapping peptides (15-mers overlapping by 12) covering 7 full-length HIV-1 gp160 Env consensus sequences (Clades A, B, C, D, Group M, CRF1 and CRF2)(46). Sequences of peptides contained in the peptide library have been previously published (47). Three identical subarrays, each containing the full peptide library, are printed on each slide. All serum samples were diluted 1:250 and hybridized to the slides using a Tecan HS4000 Hybridization Workstation, followed by incubation with DyLight 649-conjugated goat anti-rabbit IgG (Jackson ImmunoResearch, PA). Fluorescence intensity was measured using a GenePix 4300 scanner (Molecular Devices) and analyzed with GenePix software. Binding intensity of the post-immunization serum to each peptide was corrected with its own background value, which was defined as the median signal intensity of the prebleed serum for that peptide plus 3 times the standard error among the 3 subarrays on slide.

Surface Plasmon Resonance (SPR) test for binding avidity. SPR tests were performed as previously described on BIAcore 4000 instruments (20, 48). Binding dissociation rate constant (kd) and binding magnitude (response unit, RU) were measured for IgG purified from NHP sera,

at 200 µg/ml, against a panel of HIV-1 Env glycoproteins including ConS gp140, SF162ΔV2 gp140, MN gp120, and gp41 MN. Env proteins were immobilized as previously described, and avidity score was calculated as RU/kd (20).

Neutralization assays. Virus neutralization assays were performed on TZM-bl cell line, using replication competent or pseudotyped viruses grown in human peripheral blood mononuclear cells (PBMC) as previously described (49). Serial dilutions of serum samples were tested for neutralization of a panel of Tier 1 (SHIV-SF162P4 and SHIV-1157iEL-p, both as replication competent viruses) and Tier 2 (SHIV-SF162P3.5 and SHIV-89.6P.18, as pseudotyped viruses, and SHIV-89.6 and SHIV-1157ipd3N4, as replication competent viruses) SHIV viruses in TZM-bl cells.

ADCC assays. ADCC assays were performed as previously described by Pollara *et al.* (50), using CEM.NKR$_{CCR5}$ cells coated with recombinant HIV-1 SF162gp120 as target cells, and PBMC obtained from an HIV-seronegative donor as effector cells. The ADCC-mediating antibody titer was defined as the reciprocal of the highest dilution indicating a positive GzB response (>8% GzB activity) after background subtraction as previously described (50).

Statistical analysis. Differences in the levels of antibody responses between the 2 vaccine groups or between vaccine and control groups were tested using the Wilcoxon rank sum exact test with false discovery rate (FDR) controlled using the Benjamini–Hochberg method (51), performed with SAS. Correlations between binding antibody responses (binding magnitude from BAMA and epitope mapping assays and dissociation rate from SPR assays) and antibody functions (ADCC and neutralization assay) were tested using the Spearman correlation test with FDR controlled using the Benjamini-Hochberg method.

RESULTS

Rhesus macaques were immunized with SF162ΔV2 gp140 protein 5 times, either alone (gp140 group, 6 animals) or cross-linked with a CD4 mimetic miniprotein (gp140-M64U1 group, 6

181 animals) (Bogers *et al*, submitted). Env-specific antibody responses, including systemic and
182 mucosal binding specificities and antibody avidity, were evaluated with samples collected at wk
183 6 (2 weeks post 2nd immunization), wk 26 (2 weeks post 3rd immunization), wk38 (2 weeks post
184 4th immunization), and wk107 (time of 5th immunization that is 71 weeks after 4th immunization).
185 **Early Env-binding IgG response with gp140-M64U1 vaccine.**
186 To characterize the development of Env-specific binding antibody responses over time, we
187 tested longitudinal serum samples of the vaccinated animals for their binding to
188 SF162gp140ΔV2 (the immunogen), ConS gp140 (Group M consensus (52-54), MN gp120, and
189 MN gp41 proteins in binding antibody multiplex assays (BAMA). Among these 4 Env antigens
190 tested, the highest response was seen in binding to SF162gp140ΔV2 (the vaccine strain),
191 followed by ConS gp140. Similar kinetics were observed for the development of the Env-specific
192 IgG responses against the 4 Env antigens examined. Serum IgG specific for the Env proteins
193 were detectable as early as wk 6 (2 weeks after the 2nd immunization) for all 4 Env antigens
194 tested in both the gp140 and gp140-M64U1 groups (**Fig 1A-1D**). The responses generally
195 peaked at wk 26 (2 weeks after the 3rd immunization), with wk 38 (2 weeks after the 4th
196 immunization) levels comparable to that of wk 26 for both groups. The responses measured at
197 wk 107 (71 weeks after the 4th immunization) declined as expected, followed by a boost in the
198 responses measured at wk 113 (6 weeks after the 5th immunization) (**Fig 1A-1D**).
199 While the peak levels of binding antibody responses (wk 26 and wk 38) were generally
200 comparable between the two groups, the gp140-M64U1 group showed significantly higher
201 binding antibody responses at wk 6, revealing faster kinetics in the development of the anti-Env
202 responses. For all 4 Env proteins tested, binding by the wk 6 sera was much higher for the
203 gp140-M64U1 group compared to the gp140 group, with a FDR_*p* value (Wilcoxon rank sum
204 exact test *p* value controlled for false discovery rate (FDR) with the Benjamini-Hochberg
205 method) of 0.014 (**Fig. 1A-1D, Table 2**). Binding responses to all 4 Env proteins were again

comparable between the gp140 and the gp140-M64U1 groups after the last immunization at wk 113 (**Fig. 1A, Table 2**).

Decreased Linear C1 Epitope IgG with gp140-M64U1 vaccine.

Wk26 (2 weeks post 2nd immunization, the peak immunity time point) serum samples from all immunized animals were profiled for binding antibodies against gp160 linear epitopes using peptide microarray. The HIV-1 Env peptide library contains overlapping peptides covering 7 full-length consensus gp160 sequences (clade A, B, C, D, group M, CRF01 and CRF02). Serum IgG from both the gp140 and gp140-M64U1 groups bound epitopes in the C1, C2, V3, C4, V5 and C5 regions of gp120 (**Fig. 2A, 2B, and 2C**) and the gp41 immunodominant (ID) region of gp41 (**Fig. 2A, 2D and 2E**). The magnitude of binding to these epitopes was generally comparable between the 2 immunized groups at wk 26 (**Fig. 2A**), with the exception of epitope C1.2-binding, which was significantly higher for the gp140 group compared to the gp140-M64U1 group (FDR_*p* = 0.038; **Fig. 2B and 2C**, **Table 2**). Interestingly, this C1.2 linear epitope was identified in epitope mapping studies of the RV144 Thai trial, and plasma IgA binding to the corresponding C1 peptide covering the entire epitope region (C1_104. AE: MQEDVISLWDQSLKPCVKLTPLCV) correlated with increased risk of HIV-1 infection (*i.e.* decreased vaccine efficacy) in the secondary/exploratory immune correlate analysis of the trial (20). To further evaluate the kinetics and magnitude of this response, we measured the level of serum IgG response to linear C1_104.AE peptide over time by BAMA. Binding response against C1_104.AE was significantly higher for the gp140 group than the gp140-M64U1 group at wk26 (FDR_*p*=0.014; **Fig. 2F, Table 2**), which is consistent with the trend observed in wk26 linear epitope mapping data (**Fig. 2 A, B, and C)**. Similar to binding responses against Env proteins, binding responses to C1_104.AE peaked at wk 26 and wk 38, declined at wk107, and then increased again at wk113, after the fifth immunization.

We modeled this C1_104 epitope in the monomeric subunit of gp120 from the SOSIP Env trimer structure(55), which is representative of the pre-fusion conformation, and found that it is

exposed on the monomeric gp120 surface (**Fig. 2G**, red ribbon). In the CD4-bound state, the formation of the bridging sheet results in the C-terminal half of the C1_104 epitope bending ~90 degrees relative to the epitope in the SOSIP structure (**Fig.** 2G, pink ribbon). This bending results in a >30Å displacement in the position of the C-terminal residue of the C1_104 epitope, which in turn contacts CD4(56). Given the large conformational change and associated burial of C-terminal residues upon contacting CD4, antibodies that recognize C1_104 in the unbound conformation therefore may not be able to recognize the epitope in the CD4 bound state. While the effect of CD4 binding on the conformation of the C1_104 epitope in a V2 deleted gp140 may be different, these structural data do suggest that the CD4bs-cross-linked antigen may substantially impact exposure of the C1 epitope on the Env immunogen.

Induction of CD4 binding site (CD4bs) antibodies by vaccination.

Since the design of the gp140-M64U1 crosslinked immunogen involved potential modifications of gp120-CD4 interactions, we evaluated the level of CD4 binding site (CD4bs) and CD4-inducible (CD4i) antibodies by measuring binding of the antibodies to gp120 structures with and without mutations that are known to interfere with recognition of CD4bs and CD4i epitopes (57). In particular, the D368R mutation abrogates binding of most CD4bs antibodies to gp120 core or gp120 (28, 57-60), Δ371 abrogates binding of VRC01-like antibodies to gp120 resurfaced stabilized core (RSC3) (57, 59), and the I420R mutation abrogates binding of gp120 core to 17b-like CD4i antibodies (28, 59). With these reagents, we detected CD4bs binding antibodies (indicated by YU gp120 core WT:D368R ratios ≥ 2.5) in both vaccination groups (**Fig. 3A**) with comparable levels between the 2 groups (**Table 2**). Furthermore, VRC01-like binding antibodies (indicated by RSC3 WT:Δ371 ≥ 2.5) developed in both vaccination groups at generally comparable levels (**Fig. 3A, Table 2**). 17b-like CD4i antibodies, defined as HXB2 8b core WT:I420R ≥2.5, were not induced (**Fig. 3A**).

Early increase in antibody avidity with gp140-M64U1 vaccine.

Maturation of the vaccine-elicited antibody response through determination of HIV-1 Env antibody avidity is an indicator of the quality of the vaccine-induced antibody responses. We measured the avidity (as dissociation rate constant (off-rate), kd, and avidity score, RU/kd) of purified serum IgG (from wk 6, wk 26, wk 38, wk 107, and wk 113) for binding to SF162 gp140ΔV2 (**Fig. 3B**), MN gp120 (**Fig. 3C**), MN gp41 (**Fig. 3D)**, and ConS gp140 (**Fig. 3E**). The avidity scores of serum IgG to these antigens peaked at wk26 and wk38 (**Fig. 3F**), and off-rates dropped to lowest levels (slowest off-rates) at the same time-points (**Fig. 3B-3F**). At wk 6, off-rate for SF162 gp140ΔV2 was significantly slower in the gp140-M64U1 group compared to the gp140 group (median 1.7×10^{-4} versus 1.0×10^{-3} S^{-1} for gp140-M64U1 and gp140 groups respectively, FDR_*p*=0.022, **Fig. 3B, Table 2**). Off-rates were not statistically different, after FDR correction, for the two vaccine groups at wk 26, wk 38, and wk 113 (**Fig. 3B-3F, Table 2**). The longitudinal patterns of antibody off-rates and avidity score for gp41, gp120, and ConS gp140 were similar to that for SF162 gp140ΔV2, with the gp140-M64U1 group trending toward having a slower off-rate (**Fig. 3C,3D, and 3E**) and higher avidity score (**Fig 3F**) than the gp140 group.

Serum IgG Env binding avidity and magnitude correlate with ADCC and neutralization. We further explored correlations between binding antibody properties (binding MFI and off-rates) and antiviral functions (neutralization and ADCC) of antibodies elicited in the study. Vaccinations elicited low to moderate levels of neutralizing antibodies against SF162P4, with titers ranging from <10 to 4403 at the peak neutralizing activity time point of wk 38 (post 3rd immunization) in most animals (Bogers *et al*, submitted). Neutralization of SHIV SF162P4 at wk 38 was found to correlate significantly with wk 38 serum IgG binding to SF162 gp140ΔV2 (FDR_*p*=0.003, Spearman r=0.97; **Fig. 4A and Table 3**). Wk 38 neutralization of SHIV SF162P4 was also found to correlate with a faster off-rate for SF162 gp140ΔV2 at wk 6 (FDR_*p*=0.006, Spearman r=0.87; **Fig. 4B**) which indicated an inverse correlation with avidity;

however wk 38 neutralization was not significantly correlated with contemporaneous (wk 38) off-rate for SF162 gp140ΔV2 (**Table 3**).

Both vaccine groups developed strong ADCC activity measured with SF162 gp120-coated cells, which peaked at wk26 after the 2nd immunization with titers up to 19,024 (Bogers *et al*, submitted). ADCC titers were significantly higher for the gp140-M64U1 group compared to the gp140 group (FDR_*p* = 0.014) at wk 26, and trended higher at wk 113 (**Table 2**). Correlation analysis revealed that ADCC activity at wk 26 (post 3rd immunization) was not correlated with either contemporary (wk26) binding magnitude or avidity for SF162 gp140ΔV2, but rather correlated with wk6 (post 2nd immunization) serum IgG binding (FDR_*p*=0.003, Spearman r=0.90; **Fig. 4C**) and avidity (FDR_*p*=0.035, Spearman r=-0.73 for off-rate; **Fig. 4D** and **Table 3**) for SF162 gp140ΔV2, indicating that binding antibody responses early on may predict later antibody functions following further immunizations.

Low level of serum IgA elicited.

Env-specific IgA responses were evaluated in longitudinal serum samples. The overall magnitudes of HIV-1 Env serum IgA responses were much lower than serum IgG responses (**Fig. 5A vs. Fig. 1A**), with IgA binding positivity rates of 66.7% and 66.7% at wk 26 for SF162 gp140ΔV2 for gp140 and gp140-M64U1 groups, respectively, compared to 100% and 100% for IgG binding to SF162 gp140ΔV2 at wk 26. Similar to serum IgG responses, serum IgA binding to SF162 gp140ΔV2 peaked earlier for the gp140-M64U1 group, at wk 6, compared to wk 26 for the gp140 group (**Fig. 5A**). However, no significant difference between the two groups in the magnitude of responses was detected for wk6 or for any time point (**Fig. 5A, Table 2**).

Vaccine-elicited mucosal antibody responses.

Nasal and rectal samples were collected from vaccinated animals at wk 38. Env-specific IgG responses were evaluated in these mucosal samples using BAMA (29, 43).Binding magnitude (MFI) was normalized to total recovered rhesus IgG concentration (μg/ml) in each mucosal sample to account for sampling variations. Total rhesus IgG ranged from <0.5-109 μg/ml

(median 9.1 µg/ml) and <0.5-165 µg/ml (median 9.9 µg/ml) for nasal and rectal samples, respectively. We detected Env-specific IgG against SF162 gp140ΔV2, MN gp120, and MN gp41 in nasal washes from both the gp140 and gp140-M64U1 groups with comparable magnitudes (**Fig. 5B**, and data not shown). When compared to the mock immunized control animals, nasal samples from the gp140 group showed significantly higher levels of SF162 gp140ΔV2 specific antibodies (FDR_*p*=0.022, **Table 2**). The specific IgG binding of the rectal washes from the vaccinated animals to these Env proteins was not statistically different from that of control animals (data not shown). We further examined the correlation between IgG responses in the serum and the mucosal compartments and found a lack of significant correlation between serum and nasal IgG responses for binding to SF162 gp140ΔV2 (**Fig. 5C**), indicating that these are distinct immune measurements.

DISCUSSION

Here we report on the detailed binding specificities, avidity, kinetics and functional correlations of antibodies generated by immunization of rhesus macaques with an HIV-1 envelope protein (SF162ΔV2 gp140) cross-linked with a CD4 mimetic miniprotein, M64U1 (Bogers *et al*, submitted). Our findings demonstrate that cross-linking of the CD4 mimetic M64U1 with gp140 significantly impacts the kinetics, binding specificity, avidity and ADCC activity of the vaccine-elicited antibodies compared to that of gp140 protein alone. Comparison of the binding antibody responses between the gp140 and the gp140-M64U1 groups revealed an accelerated development of anti-Env binding responses in the gp140-M64U1 group, as indicated by higher binding to gp120 and gp140 Env proteins compared to the gp140 alone group at wk 6 (post 2nd immunization) (**Fig.1, Table 2**). However, Env binding responses became comparable by the time antibody responses peaked (at wk 26 and wk 38, post 3rd and 4th immunization, respectively), whereas binding to a linear C1 epitope was higher for the gp140 group compared

to the gp140-M64U1 group at wk 26. Antibody responses against M64U1 or CD4 were not measured in this current study. Follow-up studies could examine whether anti-immunogen responses were elicited and could have impacted gp140 antibody responses in the gp140-M64U1 group following later boosts.

In previous study in rabbits (42), the gp140-M64U1 complex elicited significant levels of CD4i antibodies as measured by absorption/depletion with gp120 proteins carrying the I420R mutation, which is critical for binding by 17b-like CD4i antibodies, and by neutralization of a HIV-1 virus with and without the presence of soluble CD4. In the current NHP study, no significant 17b-like CD4i antibody responses were detected in either the gp140 or the gp140-M64U1 group when examining the differential binding of serum to gp120 core protein with and without the I420R mutation (**Fig. 3A**). Another difference between the previous rabbit study and the current macaque study is the higher levels of neutralizing antibodies directed to the CD4i epitopes observed in the rabbit study following gp140-M64U1 immunization but not the current macaque study (Bogers *et al.*, submitted). Apart from differences in study methods, species differences may play a role in the difference observed. Macaques have intrinsic expression of CD4 molecules along with other surface molecules including co-receptor and DC-SIGNs (61-63) that could interact with and SIV and HIV Env, which likely affects the responses of macaques to a miniCD4-crosslinked Env. One concern for the use of CD4 mimetic proteins in vaccine regimens is the potential effect on the development of CD4bs antibodies. Broadly neutralizing CD4bs antibodies have been shown to recognize a site of “vulnerability” on the HIV-1 Env (64). Binding antibodies directed to CD4bs are commonly induced in HIV infection (57), but unfortunately those with broadly neutralizing activity seem to develop in a smaller subset of individuals (57, 65). CD4bs antibodies were detected in the gp140 group in the rabbit study (42). In the current study, we also found comparable levels of CD4bs antibodies in both the gp140 and the gp140-M64U1 groups (**Fig. 3A**).

One surprising finding in this study is the impact of M64U1-Env crosslinking on the kinetics, specificity, and avidity of antibody responses. Both the binding magnitude and avidity of the Env-specific antibodies were significantly higher (FDR_*p*=0.014) for the gp140-M64U1 group at wk 6 (post 2nd immunization), although the two groups either were comparable or the gp140 group trended higher than the gp140-M64U1 group at later time points (**Fig. 1A-1D, and Fig. 3C, Table 2**). The mechanisms for the faster development of antibody responses in the gp140-M64U1 group are not clear and warrant further investigation, including whether crosslinking of M64U1 and gp140 can affect the stability and *in vivo* trafficking of the Env protein, and how the crosslinking with M64U1 affects the interaction of Env with cells of both the adaptive and innate immune systems. In particular, exploring of the B cell responses in this macaque study revealed higher proportions of Env-specific B cells in peripheral blood mononuclear cells (PBMC) (Bogers *et al.*, submitted). Bogers *et al.* hypothesized that crosslinking with M64U1 interferes with CD4 receptor engagement, thus improving CD4 T cell-dependent immune responses.

In contrast to the binding results with the Env proteins, binding to a C1 epitope, C1_104: MQEDVISLWDQSLKPCVKLTPLCV (sequence matches that of AE clade consensus), was significantly higher for the gp140 group compared to the gp140-M64U1 group at the peak immunity time point of wk 26, as shown by both linear epitope mapping microarray and by BAMA (**Fig. 2A, 2B, and 2F, Table 2**). Plasma IgA responses to this same epitope were positively correlated with HIV-1 risk in the human RV144 vaccine clinical trial (20). Quantification of the anti-C1.2 IgA response was not possible in this study due to the low levels of overall IgA responses. Characterization of IgA responses against this C1 epitope and its correlation with ADCC response warrant further investigation. In addition, even though conformational C1-binding IgA has been indicated as potentially blocking IgG-mediated ADCC activity (66) and monoclonal IgG antibodies targeting conformational C1 epitopes can synergize with V2

385 antibodies for increased ADCC and neutralizing activities (50), the role of C1-linear binding IgG
386 in vaccine protection is not yet understood.

387 Another interesting finding in the study was the significantly higher ADCC activity in the
388 sera of animals in the gp140-M64U1 group at wk26 (Bogers *et al*., submitted, and **Table 2**).
389 ADCC activity was not measured for wk 6 serum, the only time point where Env-binding
390 magnitude was higher in the gp140-M64U1 group compared to the gp140 group. ADCC activity
391 at wk 26 significantly correlated with wk6 Env binding magnitude and off-rate (**Fig. 4C and D**),
392 but not with wk26 (contemporary) binding magnitude or off-rate (**Table 3**). The brisk and avid
393 antibody response may be a biomarker for another underlying (and unmeasured) mechanism
394 that led to enhanced ADCC function or alternatively, the early antibody response directly
395 impacted the immune mechanisms resulting in higher ADCC function. Interestingly, ADCC
396 activity was also found to correlate with proportions of Env-specific B cells in peripheral blood in
397 the same study (Bogers *et al.*, submitted). Wk38 serum neutralizing activity, on the other hand,
398 correlated with contemporary IgG binding magnitude (**Fig. 4A**) but not the contemporary IgG
399 Env avidity; it also correlated with a faster off-rate (indicating lower avidity) at the earlier time
400 point of wk6 (**Fig. 4B**) The discordant correlations of ADCC and neutralizing activities with
401 binding and avidity are in agreement with the observations from Guan *et al.* (67), suggesting
402 that different Env specificities are involved in ADCC and neutralizing anti-viral functions.
403

404 Env-specific antibodies were detected in nasal samples in both the gp140 and gp140-
405 M64U1 groups, with no difference in IgG levels between groups. The level of Env-specific IgG in
406 the nasal compartment did not correlate with serum IgG. This could be explained by selective
407 transportation of serum IgG into mucosal compartments, variation in transportation efficiency
408 among animals, or local production of IgG at the mucosal compartments. The Env gp140 used
409 in this vaccine study does not contain V2. This was based on an earlier finding of higher titers of
410 cross-reactive neutralizing antibodies in rhesus macaques immunized with SF162 V2-loop

deleted gp140 compared to those immunized with SF162 gp140 (33, 68). In light of the RV144 immune correlation found between plasma anti-V2 IgG and decreased risk of infection (20), further studies to improve upon this vaccine platform could include the addition of the V2 region in the vaccine immunogen to enable induction of V2-specific responses.

In summary, data from this study indicate that immunizing with an Env protein cross-linked to the CD4 mimetic miniprotein (M64U1) induced accelerated Env binding magnitude and avidity (as early as 2 weeks post 2nd immunization). In addition, crosslinking of gp140 with M64U1 modulated particular epitope specificities of antibody responses, such as inducing higher C1_104.AE responses in the gp140 group, likely due to alterations in the envelope structure that modulate exposure of this region upon CD4 binding. Lastly, ADCC activity at peak immunity time points (which were higher for the gp140-M64U1 group compared to the gp140 group) correlated with the magnitude and avidity of Env binding responses at an earlier time point before the ADCC and binding antibody responses reached peak levels. Taken together, these data indicate that structural modification of HIV-1 Envelope immunogens by mimicking the CD4 bound state can modulate epitope exposure in a way that substantially impacts the specificity and function of the elicited antibody responses.

Funding Information

This work was supported by the National Institutes of Health (NIH), National Institute of Allergy and Infectious Diseases (NIAID) grants, Center for HIV/AIDS Vaccine Immunology (CHAVI)/ HIV Vaccine Trials Network (HVTN) Early Stage Investigator (ESI) Award (U19AI067854, UM1AI068618), (HHSN27201100016C), 1P01AI120756 and the NIH NIAID Duke Center for AIDS Research Immunology Core P30 AI 64518. The NHP study was funded by NIH PO1 AI066287-02.

Acknowledgements

We thank Judith Lucas and Glenn Overman (Duke University) for technical assistance; Dr. Nathan Vandergrift (Duke Human Vaccine Institute Biostatistics Center) for statistical oversight; Drs. Hua-Xin Liao and Barton Haynes for envelope proteins; and Dr. Bette Korber (Los Alamos National Laboratory) for the design of the peptide sequences included in the microarray.

Figure Legends

Figure 1. Longitudinal binding antibody responses for SF162 gp140ΔV2 (vaccine strain) (**A**), ConS gp140 (**B**), MN gp120 (**C**), and MN gp41 (**D**). Shown are MFI binding values within the linear range of the assay for each antigen (1:400 for SF162 gp140ΔV2 and MN gp41; 1:80 for ConS gp140 and MN gp120). The gp140 group is shown in blue, and the gp140-M64U1 group in red. For improved data visualization of data points with similar magnitude, the x-axis is plotted categorically with staggered symbols so each data point is visible. One animal in the gp140-M64U1 died before wk107, and serum samples were not available for another 3 animals in the gp140-M64U1 group at wk107, therefore leaving 2 data points for wk107 and 5 data points for the gp140-M64U1 group. Green arrows below x-axis indicate time of vaccinations. FDR_*p*: Wilcoxon rank sum exact test *p* value controlled for false discovery rate (FDR) with the Benjamini-Hochberg method. * indicate FDR_*p*<0.05.

Figure 2. Linear epitope specificity of serum IgG by epitope mapping (**A-E**) and BAMA (**F**). Wk 26 mean binding intensity values of serum IgG for the gp140 only (B, D) and gp140-M64U1 (C,E) groups are shown for overlapping peptides of 7 consensus gp120 (B,C) and gp41 (D, E) sequences, respectively. Different colors represent different clade/circular recombinant forms (CRFs). Epitope regions identified in the study are indicated with text over horizontal bars in

plots. (**A.**) Magnitude of binding to each epitope, calculated as the highest binding to a single peptide within each epitope region, wherein percentage numbers listed under each epitope are the response rates to the epitope by the 2 groups (gp140 vs. gp140-M64U1). The peptide ranges for the epitopes are: C1.1: #16-21; C1.2: #32-39; C2: #65-68; V3: #97-104; C4: #133-139; V5-C5: #147-151; C5.1: #152-159; C5.2: #161-163; gp41-ID: #187-194. Sequences for all peptides have been previously published (47). Longitudinal binding to C1_104.AE peptide (corresponds to C1.2 epitope in epitope mapping) was measured by BAMA and is shown in panel F. Green arrows indicate time of immunizations. (**G.)** Structural modeling of the conformational change of the C1 epitope upon CD4 binding. The C1_104 epitope bends ~90 degrees from the unliganded gp120 conformation (gp120 monomer from SOSIP Env trimer; PDB 4TVP; beige) to the CD4 liganded gp120 conformation (PDB 4RQS; light blue). Binding of CD4 (PDB 4QRS; green) results in a >30Å displacement of the C-terminal residue (stick representation) between the C1_104 epitope in the unliganded gp120 (red) versus the CD4 bound C1_104 epitope (magenta).

Figure 3. CD4bs and CD4i specificity (**A**) and off-rate measurements for SF162 gp140ΔV2 (**B**), MN gp120, **(C**), MN gp41 (**D**), and ConS gp140 (**E**) in the 2 vaccine groups, and the group mean off-rates and avidity score values measured by SPR are shown (**F**). The cutoff for the CD4bs and CD4i differential binding assay (A) is 2.5-fold. For the CD4bs/CD4i differential binding assay, b12 (CD4bs mAb) was used as positive control for YU gp120 Core WT:D368R differential binding and RSC3 WT:Δ371 differential binding (57), and 17b (CD4i mAb) was used as positive control for HXB2 8b core WT:I420R differential binding (28, 57). Serum samples were tested at 1:400. Control mAbs b12 and 17b were tested as 25 and 50 µg/ml, respectively. All baseline serum samples were negative for binding to both the WTs and mutants in this test

panel. Green arrows indicate times of immunizations. FDR_*p*: Wilcoxon rank sum exact test *p* value controlled for false discovery rate (FDR) with the Benjamini-Hochberg method. * indicate FDR_*p*<0.05. Between-group comparison test results are shown in Table 2.

Figure 4. Correlation of neutralization (**A**,**B**) and ADCC (**C**,**D**) activities with serum IgG binding magnitudes (A&C) and serum IgG avidity (B&D). Spearman correlation analysis was performed using SAS, and p values are FDR corrected across all between-group comparison tests (Table 2) and this correlation test (Table 3). ** FDR_*p*<0.01; * FDR_*p*<0.05.

Figure 5. Longitudinal binding of serum IgA to SF162 gp140ΔV2 (**A**), wk 38 nasal IgG binding to SF162 gp140ΔV2 (**B**), and correlation between serum and nasal IgG binding to SF162 gp140ΔV2 at wk 38 (**C**). MFI binding values shown for IgA binding are from 1:80 serum dilution. Binding specificities for nasal samples were normalized by total IgG concentration in each sample. Green arrows indicate time of immunizations *FDR_*p*<0.05 (Wilcoxon Rank Sum Exact Test, FDR correction with Benjamini & Hochberg method).

Table 1. Immunization Schedule

Group	Immunogen	Dose (mg)	Adjuvant	Route	Time (Weeks)	# of animals
1	SF162 gp140ΔV2	100	MF59	IM	0, 4, 24, 36, 107	N=6
2	M64U1	50	MF59	IM	0, 4, 24, 36, 107	N=6
3	M64U1-SF162 gp140ΔV2	100	MF59	IM	0, 4, 24, 36, 107	N=6
4	---	---	MF59	IM	0, 4, 24, 36, 107	N=6

Table 2. Between group comparisons with False Discovery Rate [FDR] controlled p values.

Measurement	Raw_*p*	FDR_*p*
Serum IgG Binding BAMA (MFI), gp140 vs gp140-M64U1		

	SF162 gp140ΔV2 /wk6	**0.002**	**0.014***
	SF162 gp140ΔV2 /wk26	0.485	0.614
	SF162 gp140ΔV2 /wk38	**0.026**	0.071
	SF162 gp140ΔV2 /wk113	**0.017**	0.052
	ConS gp140 /wk6	**0.002**	**0.014***
	ConS gp140 /wk26	0.818	0.897
	ConS gp140 /wk38	**0.015**	0.052
	ConS gp140 /wk113	**0.017**	0.052
	MN gp120 /wk6	**0.002**	**0.014***
	MN gp120 /wk26	0.818	0.897
	MN gp120 /wk38	0.093	0.189
	MN gp120 /wk113	**0.030**	0.075
	MN gp41 /wk6	**0.002**	**0.014***
	MN gp41 /wk26	0.180	0.277
	MN gp41 /wk38	0.180	0.277
	MN gp41 /wk113	0.126	0.231
	C1_104.AE /wk6	0.180	0.277
	C1_104.AE /wk26	**0.002**	**0.014***
	C1_104.AE /wk38	**0.015**	0.052
	C1_104.AE /wk113	0.082	0.180
Serum IgG Avidity SPR (off-rate, kd), gp140 vs gp140-M64U1			
	SF162 gp140ΔV2 /wk6	**0.004**	**0.022***
	SF162 gp140ΔV2 /wk26	0.699	0.813
	SF162 gp140ΔV2 /wk38	**0.041**	0.098
	SF162 gp140ΔV2 /wk113	**0.017**	0.052
[$]*Serum IgG ADCC (Titer), gp140 vs gp140-M64U1*			
	SF162 gp140ΔV2 /wk26	**0.002**	**0.014***
	SF162 gp140ΔV2 /wk113	0.126	0.231
[$]*Serum Neutralization (ID50), gp140 vs gp140-M64U1*			
	SHIV-SF162P4 /wk38	**0.026**	0.071
	SHIV-SF162P4 /wk42	0.506	0.628
	SHIV-SF162P4 /wk113	0.126	0.231
Serum Linear Epitope Mapping (Signal Intensity), gp140 vs gp140-M64U1			
	C1.1 /wk26	**0.028**	0.073
	C1.2 /wk26	**0.009**	**0.038***
	C2 /wk26	0.318	0.422
	V3 /wk26	0.937	0.948
	C4 /wk26	0.387	0.502
	V5-C5 /wk26	0.242	0.343
	C5.1 /wk26	0.180	0.277
	C5.2 /wk26	0.937	0.948

	gp41-ID /wk26	0.240	0.343
	gp160 total /wk26	0.093	0.189
CD4bs panel BAMA (WT:mutant ratio), gp140 vs gp140-M64U1			
	RSC3 WT:Δ371 /wk26	0.536	0.650
	YU gp120 core WT:D368R /wk26	**0.043**	0.099
Serum IgA Binding BAMA (MFI), gp140 vs gp140-M64U1			
	SF162 gp140ΔV2 /wk6	0.180	0.277
	SF162 gp140ΔV2 /wk26	0.937	0.948
	SF162 gp140ΔV2 /wk38	0.310	0.420
	SF162 gp140ΔV2 /wk113	0.247	0.343
Nasal IgG Binding BAMA (Specific Activity), gp140 vs gp140-M64U1			
	SF162 gp140ΔV2 /wk38	0.132	0.235
Nasal IgG Binding BAMA (Specific Activity), gp140 vs mock control			
	SF162 gp140ΔV2 /wk38	**0.004**	**0.022***
Nasal IgG Binding BAMA (Specific Activity), gp140-M64U1 vs M64U1 control			
	SF162 gp140ΔV2 /wk38	**0.015**	0.052

[$]Quantification of neutralization and ADCC responses are reported by Bogers *et al.* (submitted).
Raw_*p*: Wilcoxon Rank Sum Exact Test [p-value], not corrected for multiple comparisons.
FDR_*p*: Controlling the False Discovery Rate, FDR_*p* values are calculated according to Benjamini & Hochberg (1995). FDR was performed across Wilcoxon Rank Sum tests in Table 2 and Spearman correlation test in Table 3 (57 tests total).
P values in bold font are <0.05.
* Significant difference between groups (FDR_*p* <0.05).

Table 3. Spearman correlation test with False Discovery Rate (FDR) control for correlation between antibody functions (ADCC or neutralization) and binding antibody responses (avidity or IgG binding), and between nasal and serum IgG responses.

Parameter 1	**Parameter 2**	**Raw_*p***	**FDR_*p***	**Spearman *r***
wk26 ADCC (linear titer)	wk6 off-rate (kd)	**0.0074**	**0.035***	-0.73
wk26 ADCC (linear titer)	wk26 off-rate (kd)	0.95	0.948	-0.021
wk26 ADCC (linear titer)	wk6 IgG binding (BAMA MFI)	**< 0.0001**	**0.003***	0.9
wk26 ADCC (linear titer)	wk26 IgG binding (BAMA MFI)	0.91	0.948	0.035
wk38 neutralization (ID_{50} titer)	wk6 off-rate (kd)	**0.0003**	**0.006***	0.87
wk38 neutralization (ID_{50} titer)	wk38 off-rate (kd)	0.75	0.850	-0.1
wk38 neutralization (ID_{50} titer)	wk6 IgG binding (BAMA MFI)	0.2	0.298	-0.4
wk38 neutralization (ID_{50} titer)	wk38 IgG binding (BAMA MFI)	**< 0.0001**	**0.003***	0.97
Nasal IgG (SA)	Serum IgG binding (MFI)	0.56	0.661	0.19

Raw_*p*: Spearman's rank correlation test [*p*-value], not corrected for multiple comparisons.

FDR_*p*: Controlling the False Discovery Rate, FDR_*p* values are calculated according to Benjamini & Hochberg (1995). FDR was performed across Wilcoxon Rank Sum tests in Table 2 and Spearman correlation test in Table 3 (57 tests total).

Bolded *p* values are <0.05.

* Significant correlation after controlling for FDR (FDR_*p*<0.05)

References

1. **Bournazos S, Klein F, Pietzsch J, Seaman MS, Nussenzweig MC, Ravetch JV.** 2014. Broadly neutralizing anti-HIV-1 antibodies require Fc effector functions for in vivo activity. Cell **158:**1243-1253.
2. **Santra S, Tomaras GD, Warrier R, Nicely NI, Liao HX, Pollara J, Liu P, Alam SM, Zhang R, Cocklin SL, Shen X, Duffy R, Xia SM, Schutte RJ, Pemble Iv CW, Dennison SM, Li H, Chao A, Vidnovic K, Evans A, Klein K, Kumar A, Robinson J, Landucci G, Forthal DN, Montefiori DC, Kaewkungwal J, Nitayaphan S, Pitisuttithum P, Rerks-Ngarm S, Robb ML, Michael NL, Kim JH, Soderberg KA, Giorgi EE, Blair L, Korber BT, Moog C, Shattock RJ, Letvin NL, Schmitz JE, Moody MA, Gao F, Ferrari G, Shaw GM, Haynes BF.** 2015. Human Non-neutralizing HIV-1 Envelope Monoclonal Antibodies Limit the Number of Founder Viruses during SHIV Mucosal Infection in Rhesus Macaques. PLoS Pathog **11:**e1005042.
3. **DeVico A, Fouts T, Lewis GK, Gallo RC, Godfrey K, Charurat M, Harris I, Galmin L, Pal R.** 2007. Antibodies to CD4-induced sites in HIV gp120 correlate with the control of SHIV challenge in macaques vaccinated with subunit immunogens. Proc Natl Acad Sci U S A **104:**17477-17482.
4. **Lu CL, Murakowski DK, Bournazos S, Schoofs T, Sarkar D, Halper-Stromberg A, Horwitz JA, Nogueira L, Golijanin J, Gazumyan A, Ravetch JV, Caskey M, Chakraborty AK, Nussenzweig MC.** 2016. Enhanced clearance of HIV-1-infected cells by broadly neutralizing antibodies against HIV-1 in vivo. Science **352:**1001-1004.
5. **Barouch DH, Liu J, Li H, Maxfield LF, Abbink P, Lynch DM, Iampietro MJ, SanMiguel A, Seaman MS, Ferrari G, Forthal DN, Ourmanov I, Hirsch VM, Carville A, Mansfield KG, Stablein D, Pau MG, Schuitemaker H, Sadoff JC, Billings EA, Rao M, Robb ML, Kim JH, Marovich MA, Goudsmit J, Michael NL.** 2012. Vaccine protection against acquisition of neutralization-resistant SIV challenges in rhesus monkeys. Nature **482:**89-93.
6. **Lai L, Kwa S, Kozlowski PA, Montefiori DC, Ferrari G, Johnson WE, Hirsch V, Villinger F, Chennareddi L, Earl PL, Moss B, Amara RR, Robinson HL.** 2011. Prevention of infection by a granulocyte-macrophage colony-stimulating factor co-expressing DNA/modified vaccinia Ankara simian immunodeficiency virus vaccine. J Infect Dis **204:**164-173.
7. **Pegu P, Vaccari M, Gordon S, Keele BF, Doster M, Guan Y, Ferrari G, Pal R, Ferrari MG, Whitney S, Hudacik L, Billings E, Rao M, Montefiori D, Tomaras G, Alam SM, Fenizia C, Lifson JD, Stablein D, Tartaglia J, Michael N, Kim J, Venzon D, Franchini G.** 2013. Antibodies with high avidity to the gp120 envelope protein in protection from simian immunodeficiency virus SIV(mac251) acquisition in an immunization regimen that mimics the RV-144 Thai trial. J Virol **87:**1708-1719.
8. **Nishimura Y, Igarashi T, Haigwood N, Sadjadpour R, Plishka RJ, Buckler-White A, Shibata R, Martin MA.** 2002. Determination of a statistically valid neutralization titer in plasma that

confers protection against simian-human immunodeficiency virus challenge following passive transfer of high-titered neutralizing antibodies. J Virol **76:**2123-2130.

9. **Hessell AJ, Rakasz EG, Tehrani DM, Huber M, Weisgrau KL, Landucci G, Forthal DN, Koff WC, Poignard P, Watkins DI, Burton DR.** 2010. Broadly neutralizing monoclonal antibodies 2F5 and 4E10 directed against the human immunodeficiency virus type 1 gp41 membrane-proximal external region protect against mucosal challenge by simian-human immunodeficiency virus SHIVBa-L. J Virol **84:**1302-1313.
10. **Baba TW, Liska V, Hofmann-Lehmann R, Vlasak J, Xu W, Ayehunie S, Cavacini LA, Posner MR, Katinger H, Stiegler G, Bernacky BJ, Rizvi TA, Schmidt R, Hill LR, Keeling ME, Lu Y, Wright JE, Chou TC, Ruprecht RM.** 2000. Human neutralizing monoclonal antibodies of the IgG1 subtype protect against mucosal simian-human immunodeficiency virus infection. Nat Med **6:**200-206.
11. **Burton DR, Hessell AJ, Keele BF, Klasse PJ, Ketas TA, Moldt B, Dunlop DC, Poignard P, Doyle LA, Cavacini L, Veazey RS, Moore JP.** 2011. Limited or no protection by weakly or nonneutralizing antibodies against vaginal SHIV challenge of macaques compared with a strongly neutralizing antibody. Proc Natl Acad Sci U S A **108:**11181-11186.
12. **Pegu A, Yang ZY, Boyington JC, Wu L, Ko SY, Schmidt SD, McKee K, Kong WP, Shi W, Chen X, Todd JP, Letvin NL, Huang J, Nason MC, Hoxie JA, Kwong PD, Connors M, Rao SS, Mascola JR, Nabel GJ.** 2014. Neutralizing antibodies to HIV-1 envelope protect more effectively in vivo than those to the CD4 receptor. Sci Transl Med **6:**243ra288.
13. **Rudicell RS, Kwon YD, Ko SY, Pegu A, Louder MK, Georgiev IS, Wu X, Zhu J, Boyington JC, Chen X, Shi W, Yang ZY, Doria-Rose NA, McKee K, O'Dell S, Schmidt SD, Chuang GY, Druz A, Soto C, Yang Y, Zhang B, Zhou T, Todd JP, Lloyd KE, Eudailey J, Roberts KE, Donald BR, Bailer RT, Ledgerwood J, Mullikin JC, Shapiro L, Koup RA, Graham BS, Nason MC, Connors M, Haynes BF, Rao SS, Roederer M, Kwong PD, Mascola JR, Nabel GJ.** 2014. Enhanced potency of a broadly neutralizing HIV-1 antibody in vitro improves protection against lentiviral infection in vivo. J Virol **88:**12669-12682.
14. **Moldt B, Rakasz EG, Schultz N, Chan-Hui PY, Swiderek K, Weisgrau KL, Piaskowski SM, Bergman Z, Watkins DI, Poignard P, Burton DR.** 2012. Highly potent HIV-specific antibody neutralization in vitro translates into effective protection against mucosal SHIV challenge in vivo. Proc Natl Acad Sci U S A **109:**18921-18925.
15. **Watkins JD, Sholukh AM, Mukhtar MM, Siddappa NB, Lakhashe SK, Kim M, Reinherz EL, Gupta S, Forthal DN, Sattentau QJ, Villinger F, Corti D, Ruprecht RM.** 2013. Anti-HIV IgA isotypes: differential virion capture and inhibition of transcytosis are linked to prevention of mucosal R5 SHIV transmission. Aids **27:**F13-20.
16. **Sholukh AM, Watkins JD, Vyas HK, Gupta S, Lakhashe SK, Thorat S, Zhou M, Hemashettar G, Bachler BC, Forthal DN, Villinger F, Sattentau QJ, Weiss RA, Agatic G, Corti D, Lanzavecchia A, Heeney JL, Ruprecht RM.** 2015. Defense-in-depth by mucosally administered anti-HIV dimeric IgA2 and systemic IgG1 mAbs: Complete protection of rhesus monkeys from mucosal SHIV challenge. Vaccine **33:**2086-2095.
17. **Barouch DH, Alter G, Broge T, Linde C, Ackerman ME, Brown EP, Borducchi EN, Smith KM, Nkolola JP, Liu J, Shields J, Parenteau L, Whitney JB, Abbink P, Ng'ang'a DM, Seaman MS, Lavine CL, Perry JR, Li W, Colantonio AD, Lewis MG, Chen B, Wenschuh H, Reimer U, Piatak M, Lifson JD, Handley SA, Virgin HW, Koutsoukos M, Lorin C, Voss G, Weijtens M, Pau MG, Schuitemaker H.** 2015. Protective efficacy of adenovirus/protein vaccines against SIV challenges in rhesus monkeys. Science **349:**320-324.
18. **McElrath MJ, Haynes BF.** 2010. Induction of immunity to human immunodeficiency virus type-1 by vaccination. Immunity **33:**542-554.
19. **Haynes BF, Burton DR.** 2017. Developing an HIV vaccine. Science **355:**1129-1130.

20. **Haynes BF, Gilbert PB, McElrath MJ, Zolla-Pazner S, Tomaras GD, Alam SM, Evans DT, Montefiori DC, Karnasuta C, Sutthent R, Liao HX, DeVico AL, Lewis GK, Williams C, Pinter A, Fong Y, Janes H, DeCamp A, Huang Y, Rao M, Billings E, Karasavvas N, Robb ML, Ngauy V, de Souza MS, Paris R, Ferrari G, Bailer RT, Soderberg KA, Andrews C, Berman PW, Frahm N, De Rosa SC, Alpert MD, Yates NL, Shen X, Koup RA, Pitisuttithum P, Kaewkungwal J, Nitayaphan S, Rerks-Ngarm S, Michael NL, Kim JH.** 2012. Immune-correlates analysis of an HIV-1 vaccine efficacy trial. N Engl J Med **366:**1275-1286.
21. **Rizzuto CD, Wyatt R, Hernandez-Ramos N, Sun Y, Kwong PD, Hendrickson WA, Sodroski J.** 1998. A conserved HIV gp120 glycoprotein structure involved in chemokine receptor binding. Science **280:**1949-1953.
22. **Salzwedel K, Smith ED, Dey B, Berger EA.** 2000. Sequential CD4-coreceptor interactions in human immunodeficiency virus type 1 Env function: soluble CD4 activates Env for coreceptor-dependent fusion and reveals blocking activities of antibodies against cryptic conserved epitopes on gp120. J Virol **74:**326-333.
23. **Xiang SH, Doka N, Choudhary RK, Sodroski J, Robinson JE.** 2002. Characterization of CD4-induced epitopes on the HIV type 1 gp120 envelope glycoprotein recognized by neutralizing human monoclonal antibodies. AIDS Res Hum Retroviruses **18:**1207-1217.
24. **Decker JM, Bibollet-Ruche F, Wei X, Wang S, Levy DN, Wang W, Delaporte E, Peeters M, Derdeyn CA, Allen S, Hunter E, Saag MS, Hoxie JA, Hahn BH, Kwong PD, Robinson JE, Shaw GM.** 2005. Antigenic conservation and immunogenicity of the HIV coreceptor binding site. J Exp Med **201:**1407-1419.
25. **Kwong PD, Wyatt R, Robinson J, Sweet RW, Sodroski J, Hendrickson WA.** 1998. Structure of an HIV gp120 envelope glycoprotein in complex with the CD4 receptor and a neutralizing human antibody. Nature **393:**648-659.
26. **Lewis GK, Fouts TR, Ibrahim S, Taylor BM, Salkar R, Guan Y, Kamin-Lewis R, Robinson JE, Devico AL.** 2011. Identification and characterization of an immunogenic hybrid epitope formed by both HIV gp120 and human CD4 proteins. J Virol **85:**13097-13104.
27. **Lusso P, Earl PL, Sironi F, Santoro F, Ripamonti C, Scarlatti G, Longhi R, Berger EA, Burastero SE.** 2005. Cryptic nature of a conserved, CD4-inducible V3 loop neutralization epitope in the native envelope glycoprotein oligomer of CCR5-restricted, but not CXCR4-using, primary human immunodeficiency virus type 1 strains. J Virol **79:**6957-6968.
28. **Li Y, Svehla K, Louder MK, Wycuff D, Phogat S, Tang M, Migueles SA, Wu X, Phogat A, Shaw GM, Connors M, Hoxie J, Mascola JR, Wyatt R.** 2009. Analysis of neutralization specificities in polyclonal sera derived from human immunodeficiency virus type 1-infected individuals. J Virol **83:**1045-1059.
29. **Tomaras GD, Yates NL, Liu P, Qin L, Fouda GG, Chavez LL, Decamp AC, Parks RJ, Ashley VC, Lucas JT, Cohen M, Eron J, Hicks CB, Liao HX, Self SG, Landucci G, Forthal DN, Weinhold KJ, Keele BF, Hahn BH, Greenberg ML, Morris L, Karim SS, Blattner WA, Montefiori DC, Shaw GM, Perelson AS, Haynes BF.** 2008. Initial B-cell responses to transmitted human immunodeficiency virus type 1: virion-binding immunoglobulin M (IgM) and IgG antibodies followed by plasma anti-gp41 antibodies with ineffective control of initial viremia. J Virol **82:**12449-12463.
30. **Thomas MA, Tuero I, Demberg T, Vargas-Inchaustegui DA, Musich T, Xiao P, Venzon D, LaBranche C, Montefiori DC, DiPasquale J, Reed SG, DeVico A, Fouts T, Lewis GK, Gallo RC, Robert-Guroff M.** 2014. HIV-1 CD4-induced (CD4i) gp120 epitope vaccines promote B and T-cell responses that contribute to reduced viral loads in rhesus macaques. Virology **471-473:**81-92.
31. **Varadarajan R, Sharma D, Chakraborty K, Patel M, Citron M, Sinha P, Yadav R, Rashid U, Kennedy S, Eckert D, Geleziunas R, Bramhill D, Schleif W, Liang X, Shiver J.** 2005. Characterization of gp120 and its single-chain derivatives, gp120-CD4D12 and gp120-M9:

implications for targeting the CD4i epitope in human immunodeficiency virus vaccine design. J Virol **79:**1713-1723.

32. **Devico A, Silver A, Thornton AM, Sarngadharan MG, Pal R.** 1996. Covalently Crosslinked Complexes of Human Immunodeficiency Virus Type 1 (HIV-1) gp120 and CD4 Receptor Elicit a Neutralizing Immune Response That Includes Antibodies Selective for Primary Virus Isolates. Virology **218:**258-263.
33. **Fouts T, Godfrey K, Bobb K, Montefiori D, Hanson CV, Kalyanaraman VS, DeVico A, Pal R.** 2002. Crosslinked HIV-1 envelope–CD4 receptor complexes elicit broadly cross-reactive neutralizing antibodies in rhesus macaques. Proceedings of the National Academy of Sciences **99:**11842-11847.
34. **Fouts TR, Tuskan R, Godfrey K, Reitz M, Hone D, Lewis GK, DeVico AL.** 2000. Expression and characterization of a single-chain polypeptide analogue of the human immunodeficiency virus type 1 gp120-CD4 receptor complex. J Virol **74:**11427-11436.
35. **Vita C, Drakopoulou E, Vizzavona J, Rochette S, Martin L, Menez A, Roumestand C, Yang YS, Ylisastigui L, Benjouad A, Gluckman JC.** 1999. Rational engineering of a miniprotein that reproduces the core of the CD4 site interacting with HIV-1 envelope glycoprotein. Proc Natl Acad Sci U S A **96:**13091-13096.
36. **Zhao Q, Ma L, Jiang S, Lu H, Liu S, He Y, Strick N, Neamati N, Debnath AK.** 2005. Identification of N-phenyl-N'-(2,2,6,6-tetramethyl-piperidin-4-yl)-oxalamides as a new class of HIV-1 entry inhibitors that prevent gp120 binding to CD4. Virology **339:**213-225.
37. **Madani N, Princiotto AM, Zhao C, Jahanbakhshsefidi F, Mertens M, Herschhorn A, Melillo B, Smith AB, 3rd, Sodroski J.** 2017. Activation and Inactivation of Primary Human Immunodeficiency Virus Envelope Glycoprotein Trimers by CD4-Mimetic Compounds. J Virol **91**.
38. **Martin G, Burke B, Thai R, Dey AK, Combes O, Ramos OH, Heyd B, Geonnotti AR, Montefiori DC, Kan E, Lian Y, Sun Y, Abache T, Ulmer JB, Madaoui H, Guerois R, Barnett SW, Srivastava IK, Kessler P, Martin L.** 2011. Stabilization of HIV-1 envelope in the CD4-bound conformation through specific cross-linking of a CD4 mimetic. J Biol Chem **286:**21706-21716.
39. **Martin L, Stricher F, Misse D, Sironi F, Pugniere M, Barthe P, Prado-Gotor R, Freulon I, Magne X, Roumestand C, Menez A, Lusso P, Veas F, Vita C.** 2003. Rational design of a CD4 mimic that inhibits HIV-1 entry and exposes cryptic neutralization epitopes. Nat Biotechnol **21:**71-76.
40. **Van Herrewege Y, Morellato L, Descours A, Aerts L, Michiels J, Heyndrickx L, Martin L, Vanham G.** 2008. CD4 mimetic miniproteins: potent anti-HIV compounds with promising activity as microbicides. J Antimicrob Chemother **61:**818-826.
41. **Stricher F, Huang CC, Descours A, Duquesnoy S, Combes O, Decker JM, Kwon YD, Lusso P, Shaw GM, Vita C, Kwong PD, Martin L.** 2008. Combinatorial optimization of a CD4-mimetic miniprotein and cocrystal structures with HIV-1 gp120 envelope glycoprotein. J Mol Biol **382:**510-524.
42. **Dey AK, Burke B, Sun Y, Sirokman K, Nandi A, Hartog K, Lian Y, Geonnotti AR, Montefiori D, Franti M, Martin G, Carfi A, Kessler P, Martin L, Srivastava IK, Barnett SW.** 2012. Elicitation of neutralizing antibodies directed against CD4-induced epitope(s) using a CD4 mimetic cross-linked to a HIV-1 envelope glycoprotein. PLoS One **7:**e30233.
43. **Yates NL, Stacey AR, Nolen TL, Vandergrift NA, Moody MA, Montefiori DC, Weinhold KJ, Blattner WA, Borrow P, Shattock R, Cohen MS, Haynes BF, Tomaras GD.** 2013. HIV-1 gp41 envelope IgA is frequently elicited after transmission but has an initial short response half-life. Mucosal Immunol **6:**692-703.
44. **Zurawski G, Shen X, Zurawski S, Tomaras GD, Montefiori DC, Roederer M, Ferrari G, Lacabaratz C, Klucar P, Wang Z, Foulds KE, Kao SF, Yu X, Sato A, Yates NL, LaBranche C, Stanfield-Oakley S, Kibler K, Jacobs B, Salazar A, Self S, Fulp J, Gottardo R, Galmin L, Weiss D, Cristillo A, Pantaleo**

G, Levy Y. 2017. Superiority in Rhesus Macaques of Targeting HIV-1 Env Gp140 to CD40 Versus LOX-1 in Combination with Replication Competent NYVAC-KC for Induction of Env-Specific Antibody and T Cell Responses. J Virol doi:10.1128/jvi.01596-16.

45. **Tomaras GD, Binley JM, Gray ES, Crooks ET, Osawa K, Moore PL, Tumba N, Tong T, Shen X, Yates NL, Decker J, Wibmer CK, Gao F, Alam SM, Easterbrook P, Abdool Karim S, Kamanga G, Crump JA, Cohen M, Shaw GM, Mascola JR, Haynes BF, Montefiori DC, Morris L.** 2011. Polyclonal B cell responses to conserved neutralization epitopes in a subset of HIV-1-infected individuals. J Virol **85:**11502-11519.

46. **Shen X, Duffy R, Howington R, Cope A, Sadagopal S, Park H, Pal R, Kwa S, Ding S, Yang OO, Fouda GG, Le Grand R, Bolton D, Esteban M, Phogat S, Roederer M, Amara R, Picker LJ, Seder RA, McElrath MJ, Barnett S, Permar SR, Shattock R, DeVico AL, Felber BK, Pavlakis GN, Pantaleo G, Korber BT, Montefiori DC, Tomaras GD.** 2015. Vaccine Induced Epitope Specific Antibodies to SIVmac239 Envelope Are Distinct from Those Induced to the HIV-1 Envelope in Non-Human Primates. J Virol doi:10.1128/jvi.03635-14.

47. **Gottardo R, Bailer RT, Korber BT, Gnanakaran S, Phillips J, Shen X, Tomaras GD, Turk E, Imholte G, Eckler L, Wenschuh H, Zerweck J, Greene K, Gao H, Berman PW, Francis D, Sinangil F, Lee C, Nitayaphan S, Rerks-Ngarm S, Kaewkungwal J, Pitisuttithum P, Tartaglia J, Robb ML, Michael NL, Kim JH, Zolla-Pazner S, Haynes BF, Mascola JR, Self S, Gilbert P, Montefiori DC.** 2013. Plasma IgG to linear epitopes in the V2 and V3 regions of HIV-1 gp120 correlate with a reduced risk of infection in the RV144 vaccine efficacy trial. PLoS One **8:**e75665.

48. **Lynch HE, Stewart SM, Kepler TB, Sempowski GD, Alam SM.** 2014. Surface plasmon resonance measurements of plasma antibody avidity during primary and secondary responses to anthrax protective antigen. J Immunol Methods **404:**1-12.

49. **Li M, Gao F, Mascola JR, Stamatatos L, Polonis VR, Koutsoukos M, Voss G, Goepfert P, Gilbert P, Greene KM, Bilska M, Kothe DL, Salazar-Gonzalez JF, Wei X, Decker JM, Hahn BH, Montefiori DC.** 2005. Human immunodeficiency virus type 1 env clones from acute and early subtype B infections for standardized assessments of vaccine-elicited neutralizing antibodies. J Virol **79:**10108-10125.

50. **Pollara J, Bonsignori M, Moody MA, Liu P, Alam SM, Hwang KK, Gurley TC, Kozink DM, Armand LC, Marshall DJ, Whitesides JF, Kaewkungwal J, Nitayaphan S, Pitisuttithum P, Rerks-Ngarm S, Robb ML, O'Connell RJ, Kim JH, Michael NL, Montefiori DC, Tomaras GD, Liao HX, Haynes BF, Ferrari G.** 2014. HIV-1 vaccine-induced C1 and V2 Env-specific antibodies synergize for increased antiviral activities. J Virol **88:**7715-7726.

51. **Benjamini Y, Hochberg Y.** 1995. Controlling the false discovery rate: a practical and powerful approach to multiple testing. Journal of the Royal Statistical Society **B 57:**289-300.

52. **Gao F, Weaver EA, Lu Z, Li Y, Liao HX, Ma B, Alam SM, Scearce RM, Sutherland LL, Yu JS, Decker JM, Shaw GM, Montefiori DC, Korber BT, Hahn BH, Haynes BF.** 2005. Antigenicity and immunogenicity of a synthetic human immunodeficiency virus type 1 group m consensus envelope glycoprotein. J Virol **79:**1154-1163.

53. **Gaschen B, Taylor J, Yusim K, Foley B, Gao F, Lang D, Novitsky V, Haynes B, Hahn BH, Bhattacharya T, Korber B.** 2002. Diversity considerations in HIV-1 vaccine selection. Science **296:**2354-2360.

54. **Liao HX, Sutherland LL, Xia SM, Brock ME, Scearce RM, Vanleeuwen S, Alam SM, McAdams M, Weaver EA, Camacho Z, Ma BJ, Li Y, Decker JM, Nabel GJ, Montefiori DC, Hahn BH, Korber BT, Gao F, Haynes BF.** 2006. A group M consensus envelope glycoprotein induces antibodies that neutralize subsets of subtype B and C HIV-1 primary viruses. Virology **353:**268-282.

55. **Pancera M, Zhou T, Druz A, Georgiev IS, Soto C, Gorman J, Huang J, Acharya P, Chuang GY, Ofek G, Stewart-Jones GB, Stuckey J, Bailer RT, Joyce MG, Louder MK, Tumba N, Yang Y, Zhang**

B, Cohen MS, Haynes BF, Mascola JR, Morris L, Munro JB, Blanchard SC, Mothes W, Connors M, Kwong PD. 2014. Structure and immune recognition of trimeric pre-fusion HIV-1 Env. Nature **514:**455-461.

56. **Kong L, Wilson IA, Kwong PD.** 2015. Crystal structure of a fully glycosylated HIV-1 gp120 core reveals a stabilizing role for the glycan at Asn262. Proteins **83:**590-596.
57. **Lynch RM, Tran L, Louder MK, Schmidt SD, Cohen M, Dersimonian R, Euler Z, Gray ES, Abdool Karim S, Kirchherr J, Montefiori DC, Sibeko S, Soderberg K, Tomaras G, Yang ZY, Nabel GJ, Schuitemaker H, Morris L, Haynes BF, Mascola JR.** 2012. The development of CD4 binding site antibodies during HIV-1 infection. J Virol **86:**7588-7595.
58. **Olshevsky U, Helseth E, Furman C, Li J, Haseltine W, Sodroski J.** 1990. Identification of individual human immunodeficiency virus type 1 gp120 amino acids important for CD4 receptor binding. J Virol **64:**5701-5707.
59. **Wu X, Yang ZY, Li Y, Hogerkorp CM, Schief WR, Seaman MS, Zhou T, Schmidt SD, Wu L, Xu L, Longo NS, McKee K, O'Dell S, Louder MK, Wycuff DL, Feng Y, Nason M, Doria-Rose N, Connors M, Kwong PD, Roederer M, Wyatt RT, Nabel GJ, Mascola JR.** 2010. Rational design of envelope identifies broadly neutralizing human monoclonal antibodies to HIV-1. Science **329:**856-861.
60. **Thali M, Olshevsky U, Furman C, Gabuzda D, Posner M, Sodroski J.** 1991. Characterization of a discontinuous human immunodeficiency virus type 1 gp120 epitope recognized by a broadly reactive neutralizing human monoclonal antibody. J Virol **65:**6188-6193.
61. **Benton PA, Timanus DK, Shearer MH, White GL, Lee DR, Kennedy RC.** 1999. Analysis of nonhuman primate peripheral blood mononuclear cells for susceptibility to HIV-1 infection and hiv coreceptor expression. Developmental & Comparative Immunology **23:**97-105.
62. **Bashirova AA, Wu L, Cheng J, Martin TD, Martin MP, Benveniste RE, Lifson JD, KewalRamani VN, Hughes A, Carrington M.** 2003. Novel member of the CD209 (DC-SIGN) gene family in primates. J Virol **77:**217-227.
63. **Unutmaz D, Xiang W, Sunshine MJ, Campbell J, Butcher E, Littman DR.** 2000. The primate lentiviral receptor Bonzo/STRL33 is coordinately regulated with CCR5 and its expression pattern is conserved between human and mouse. J Immunol **165:**3284-3292.
64. **Kwong Peter D, Mascola John R.** 2012. Human Antibodies that Neutralize HIV-1: Identification, Structures, and B Cell Ontogenies. Immunity **37:**412-425.
65. **Sather DN, Armann J, Ching LK, Mavrantoni A, Sellhorn G, Caldwell Z, Yu X, Wood B, Self S, Kalams S, Stamatatos L.** 2009. Factors associated with the development of cross-reactive neutralizing antibodies during human immunodeficiency virus type 1 infection. J Virol **83:**757-769.
66. **Tomaras GD, Ferrari G, Shen X, Alam SM, Liao H-X, Pollara J, Bonsignori M, Moody MA, Fong Y, Chen X, Poling B, Nicholson CO, Zhang R, Lu X, Parks R, Kaewkungwal J, Nitayaphan S, Pitisuttithum P, Rerks-Ngarm S, Gilbert PB, Kim JH, Michael NL, Montefiori DC, Haynes BF.** 2013. Vaccine-induced plasma IgA specific for the C1 region of the HIV-1 envelope blocks binding and effector function of IgG. Proceedings of the National Academy of Sciences **110:**9019-9024.
67. **Guan Y, Pazgier M, Sajadi MM, Kamin-Lewis R, Al-Darmarki S, Flinko R, Lovo E, Wu X, Robinson JE, Seaman MS, Fouts TR, Gallo RC, DeVico AL, Lewis GK.** 2013. Diverse specificity and effector function among human antibodies to HIV-1 envelope glycoprotein epitopes exposed by CD4 binding. Proc Natl Acad Sci U S A **110:**E69-78.
68. **Srivastava IK, Stamatatos L, Kan E, Vajdy M, Lian Y, Hilt S, Martin L, Vita C, Zhu P, Roux KH, Vojtech L, D CM, Donnelly J, Ulmer JB, Barnett SW.** 2003. Purification, characterization, and immunogenicity of a soluble trimeric envelope protein containing a partial deletion of the V2

801 loop derived from SF162, an R5-tropic human immunodeficiency virus type 1 isolate. J Virol
802 **77:**11244-11259.

803

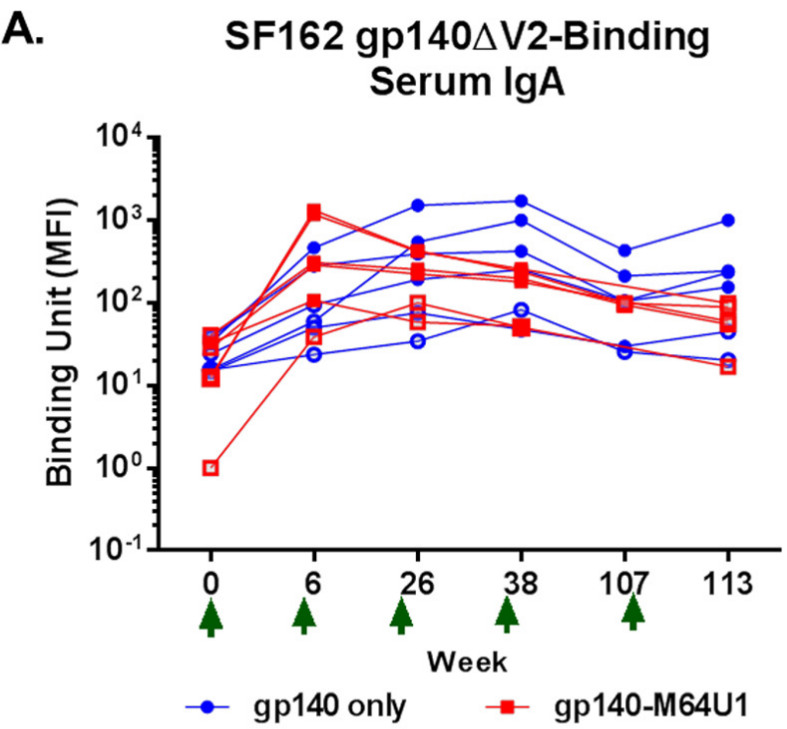
A.
SF162 gp140ΔV2-Binding Serum IgA
Binding Unit (MFI)
10^4
10^3
10^2
10^1
10^0
10^{-1}
0
6
26
38
107
113
Week
gp140 only
gp140-M64U1

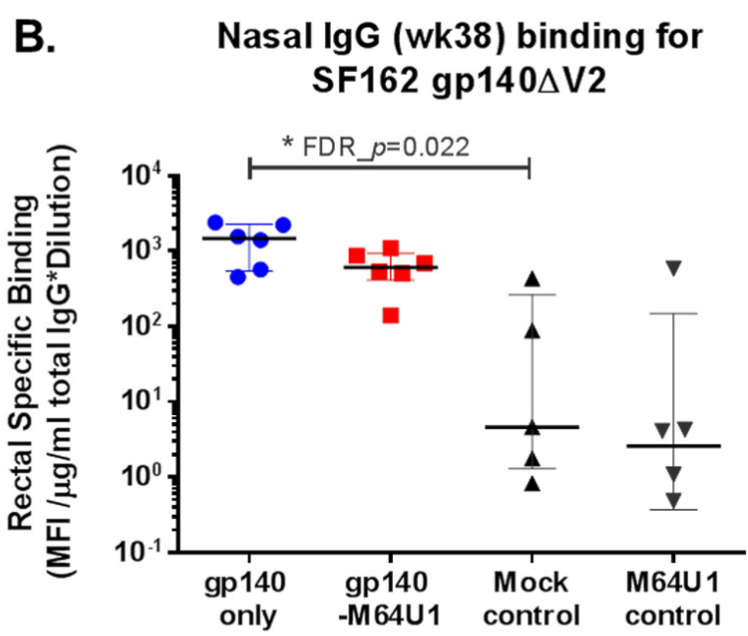
B.
Nasal IgG (wk38) binding for SF162 gp140ΔV2
* FDR_p=0.022
Rectal Specific Binding (MFI /µg/ml total IgG*Dilution)
10^4
10^3
10^2
10^1
10^0
10^{-1}
gp140 only
gp140 -M64U1
Mock control
M64U1 control

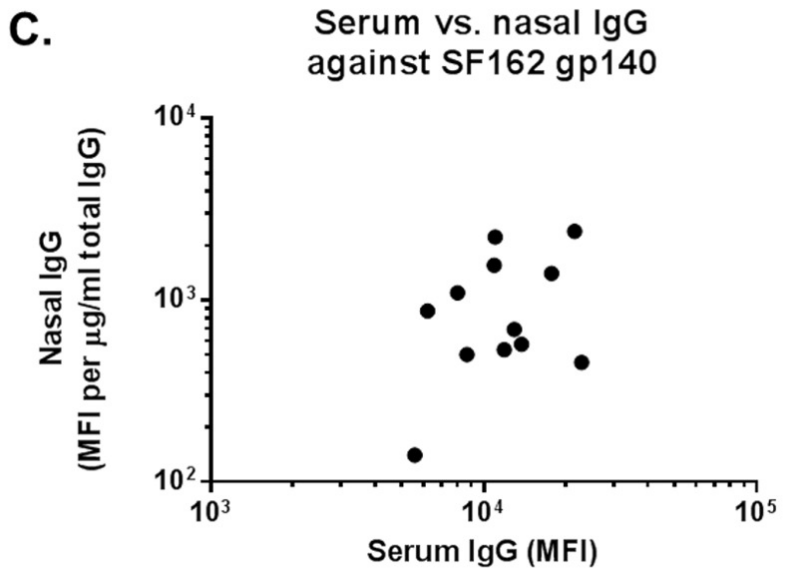
C.
Serum vs. nasal IgG against SF162 gp140
Nasal IgG (MFI per µg/ml total IgG)
10^4
10^3
10^2
10^3
10^4
10^5
Serum IgG (MFI)

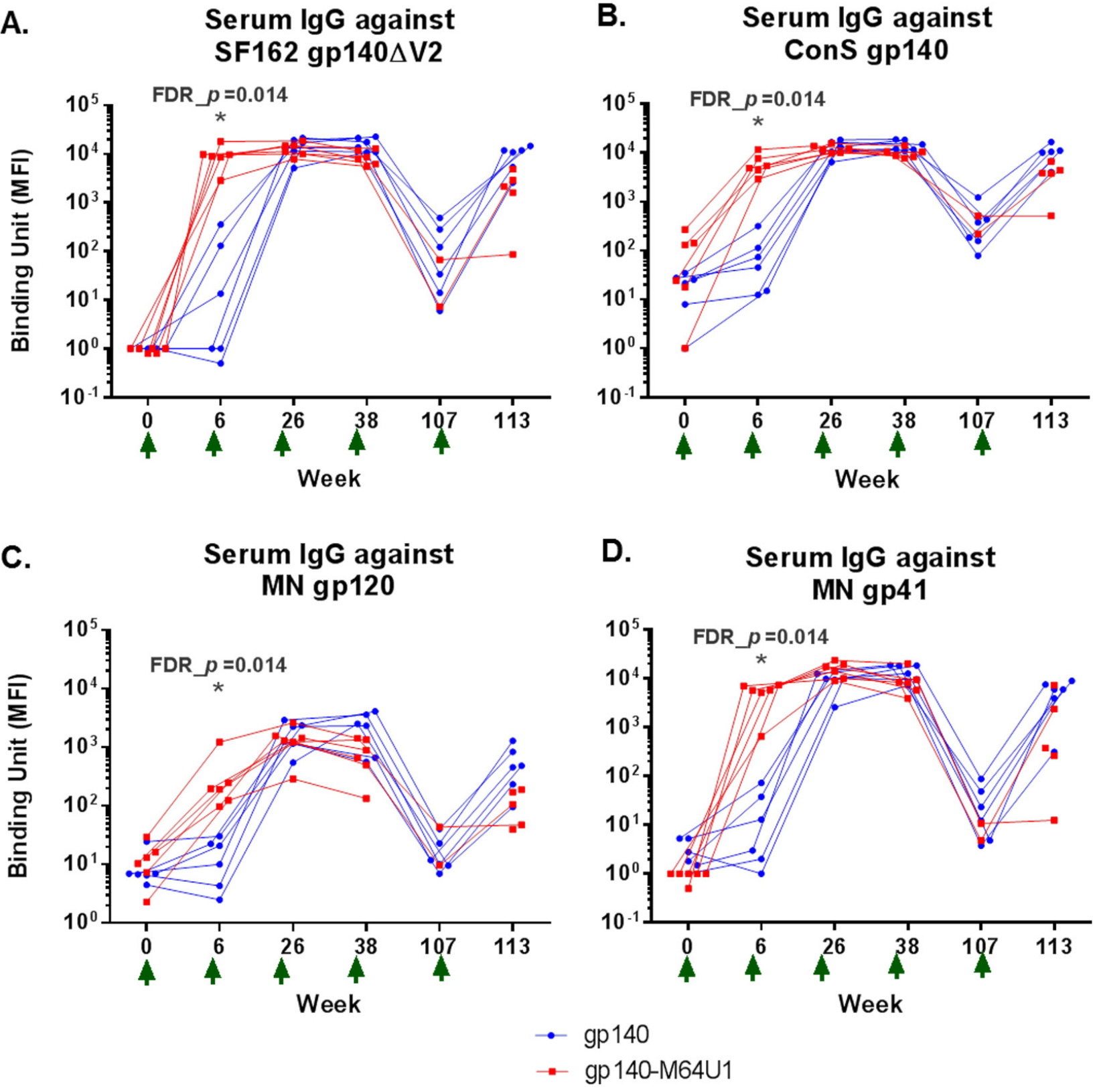
A.
Serum IgG against
SF162 gp140ΔV2
FDR_p =0.014
*
Binding Unit (MFI)
Week
B.
Serum IgG against
ConS gp140
FDR_p =0.014
*
Week
C.
Serum IgG against
MN gp120
FDR_p =0.014
*
Binding Unit (MFI)
Week
D.
Serum IgG against
MN gp41
FDR_p =0.014
*
Week
gp140
gp140-M64U1

A.

	Animal ID	C1.1 83% vs17%	C1.2* 100% vs 67%	C2 50% vs 33%	V3 100% vs100%	C4 100% vs 50%	V5 67% vs17%	C5.1 100% vs 100%	C5.2 100% vs 100%	gp41-ID 100% vs 100%
Gp140 only	Ri960903	1,025	2,340	1	63,970	28,000	1	4,393	12,541	5,744
	Ri9605031	267	8,668	1	26,599	2,413	206	2,778	3,221	6,742
	Ri9707023	349	6,368	4,056	25,637	3,583	9,981	22,094	2,484	19,878
	Ri0001081	7,392	10,015	4,507	38,191	5,553	4,857	12,623	4,864	7,169
	Ri967277	1	1,303	1	47,797	4,786	1	6,103	11,017	9,282
	Ri0007043	2,278	13,268	1,922	43,684	14,407	4,687	19,300	7,032	19,265
Gp140-M64U1	Ri0105051	1	852	814	40,427	8,256	15,885	13,724	5,797	23,059
	Ri9807263	1	1	1	35,068	10,298	1	1,196	5,104	10,090
	Ri0006311	1	1	1	52,887	1	1	1,549	8,923	36,185
	Ri9606231	1	2,346	1	37,892	1	1	3,682	4,363	8,591
	Ri9807071	1	424	227	30,055	1	1	5,720	3,244	12,850
	Ri9706291	279	267	1	38,307	6,746	1	5,064	6,562	7,246

*The difference between groups for binding to C1.2 epitope was significant, with FDR_p of 0.038.

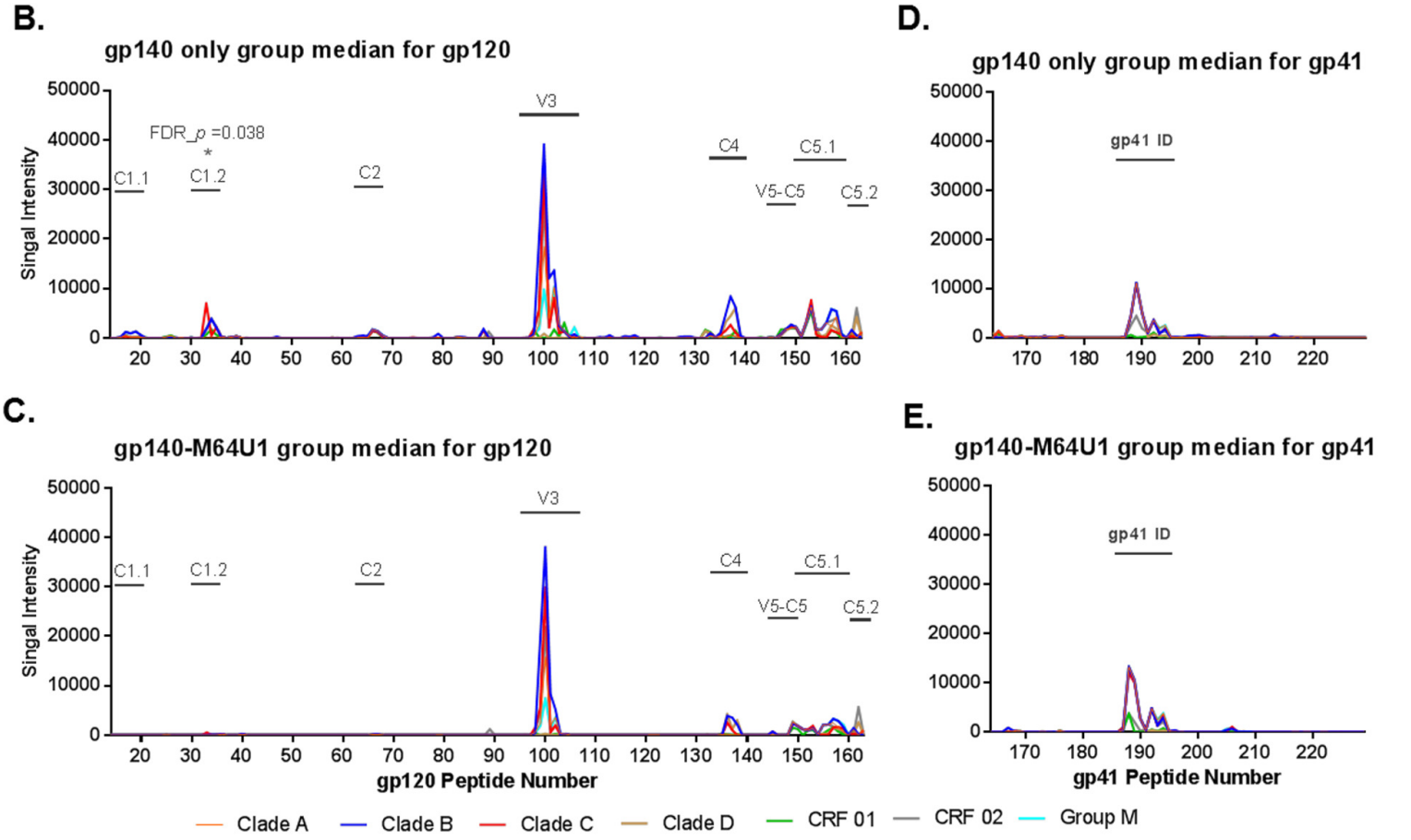

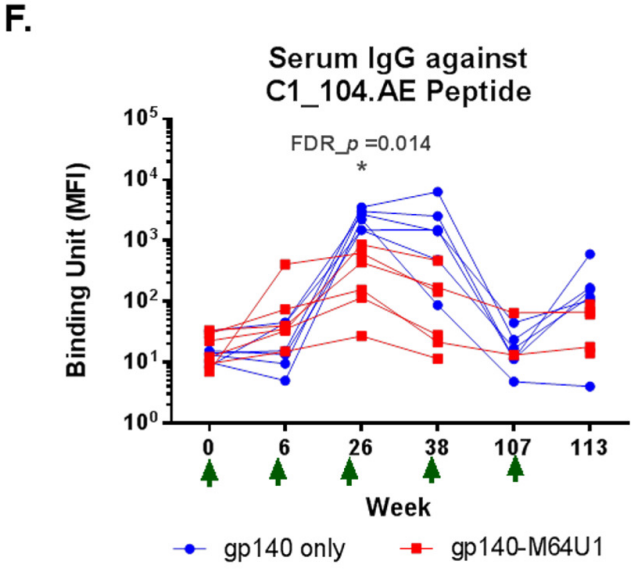

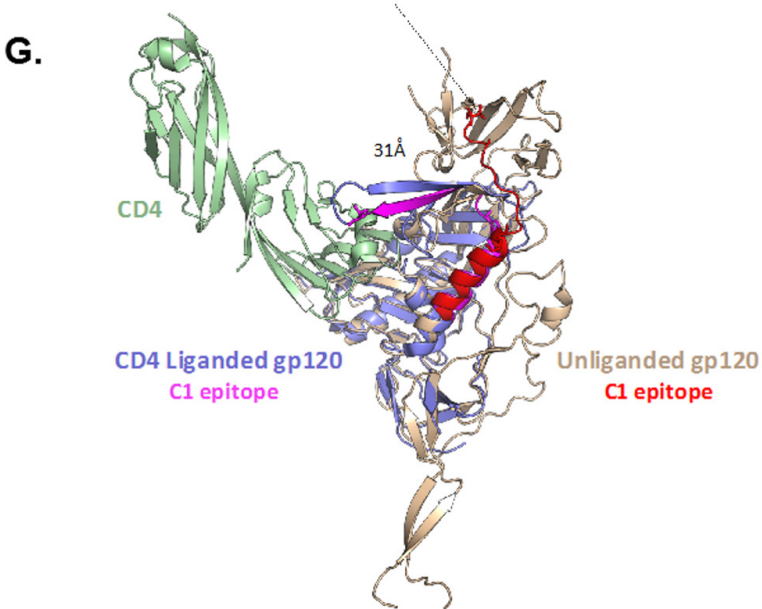

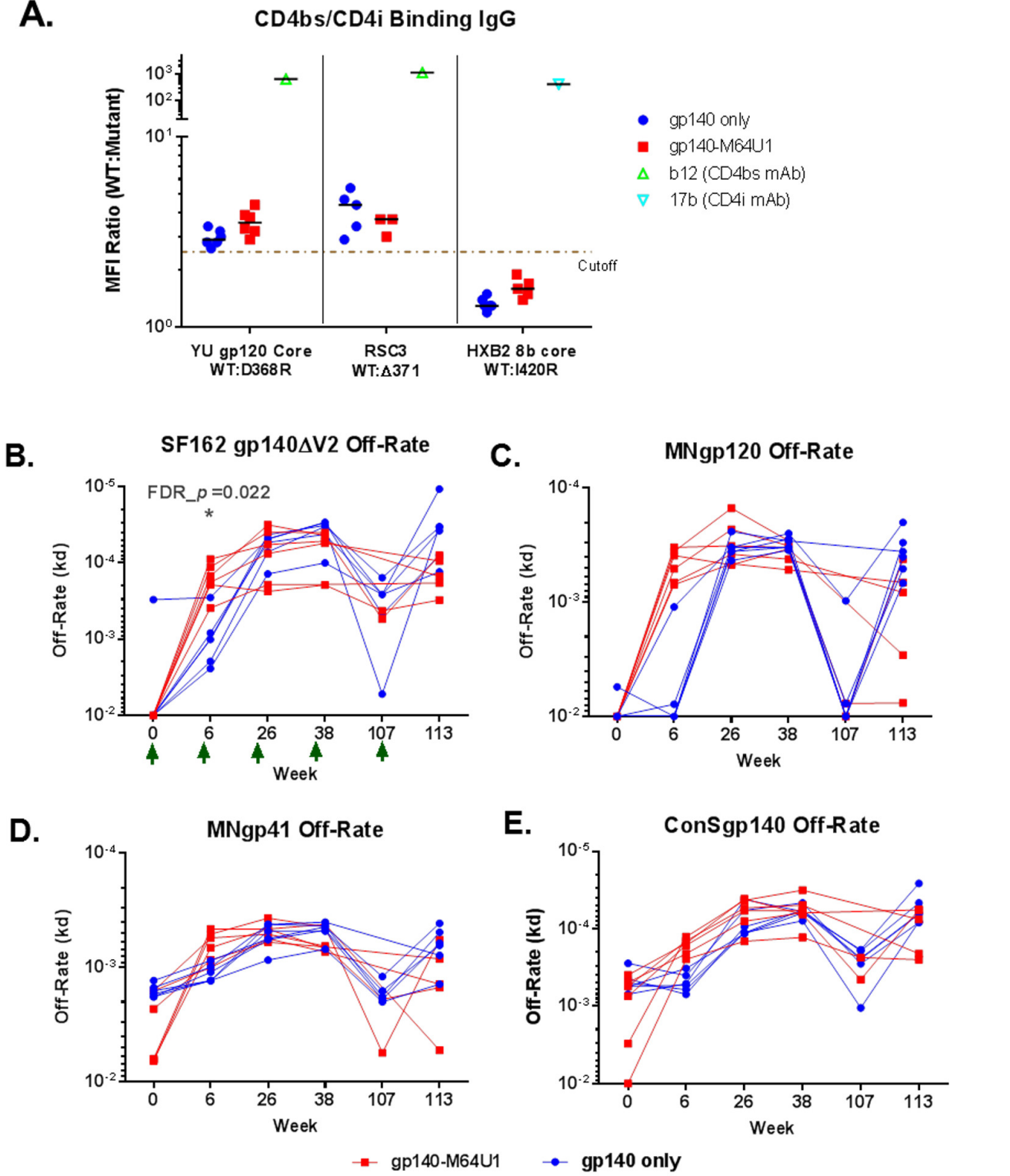

F.

Group	Dissociation constant (kd, s^{-1}) wk6	wk26	wk38	wk107	wk113	Avidity score (RU/kd) wk6	wk26	wk38	wk107	wk113
SF162 gp140ΔV2										
gp140 only	1.0E-03	6.1E-05	4.0E-05	4.4E-04	4.1E-05	5.0E+04	5.9E+06	1.1E+07	1.1E+05	6.2E+06
gp140-M64U1	1.7E-04	7.9E-05	7.5E-05	4.8E-04	1.4E-04	1.6E+06	3.8E+06	3.0E+06	4.7E+04	6.2E+05
ConS gp140										
gp140 only	5.0E-04	8.3E-05	6.0E-05	2.9E-04	5.7E-05	7.5E+04	3.6E+06	5.6E+06	1.0E+05	5.7E+06
gp140-M64U1	1.7E-04	6.3E-05	6.0E-05	3.3E-04	1.1E-04	1.2E+06	4.8E+06	3.8E+06	8.6E+04	7.7E+05
MN gp120										
gp140 only	6.6E-03	3.4E-04	3.0E-04	4.1E-03	3.8E-04	3.8E+02	1.2E+05	1.5E+05	1.0E+03	7.7E+04
gp140-M64U1	4.7E-04	3.1E-04	3.6E-04	8.8E-03	1.4E-03	5.5E+04	1.2E+05	8.1E+04	6.0E+02	2.0E+04
MN gp41										
gp140 only	1.1E-03	5.3E-04	4.8E-04	1.6E-03	6.6E-04	2.1E+04	1.4E+05	1.8E+05	1.4E+04	7.9E+04
gp140-M64U1	6.5E-04	4.8E-04	5.8E-04	3.3E-03	1.4E-03	8.7E+04	1.7E+05	1.0E+05	7.8E+03	2.8E+04

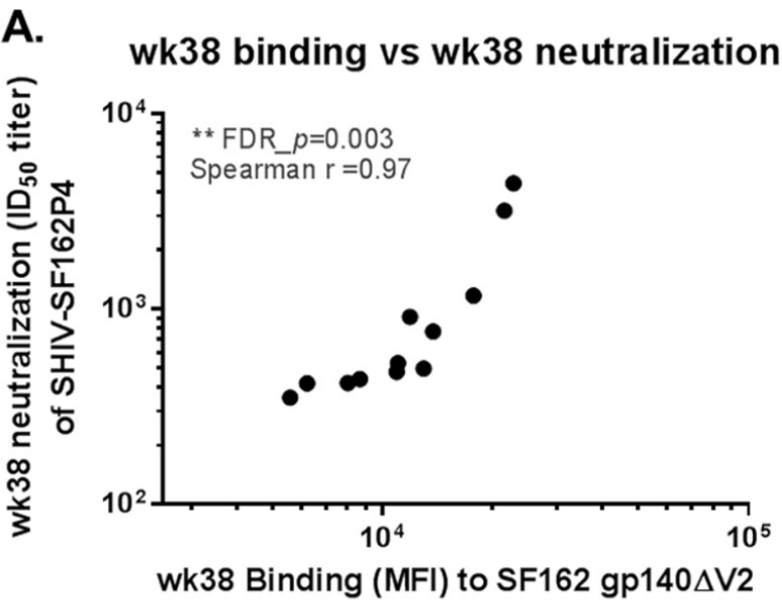
A.
wk38 binding vs wk38 neutralization
** FDR_p=0.003
Spearman r =0.97
wk38 neutralization (ID50 titer) of SHIV-SF162P4
wk38 Binding (MFI) to SF162 gp140ΔV2

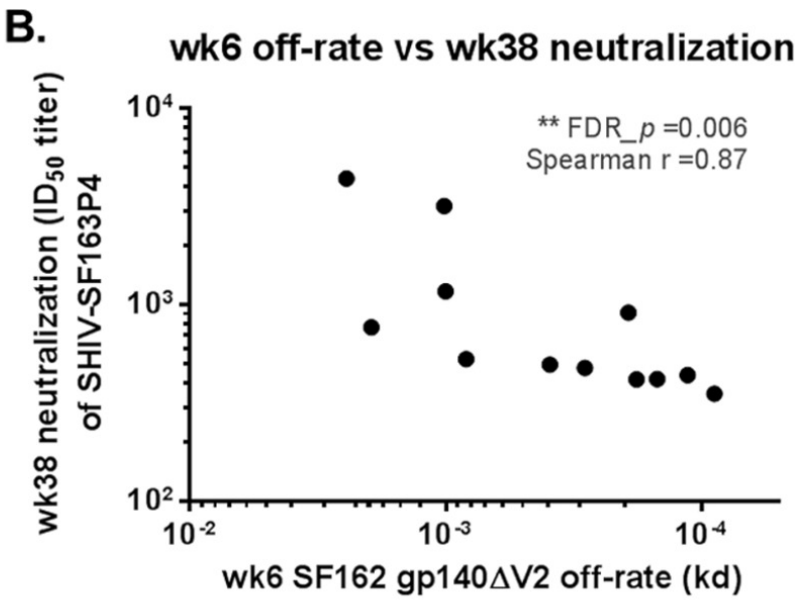
B.
wk6 off-rate vs wk38 neutralization
** FDR_p =0.006
Spearman r =0.87
wk38 neutralization (ID50 titer) of SHIV-SF163P4
wk6 SF162 gp140ΔV2 off-rate (kd)

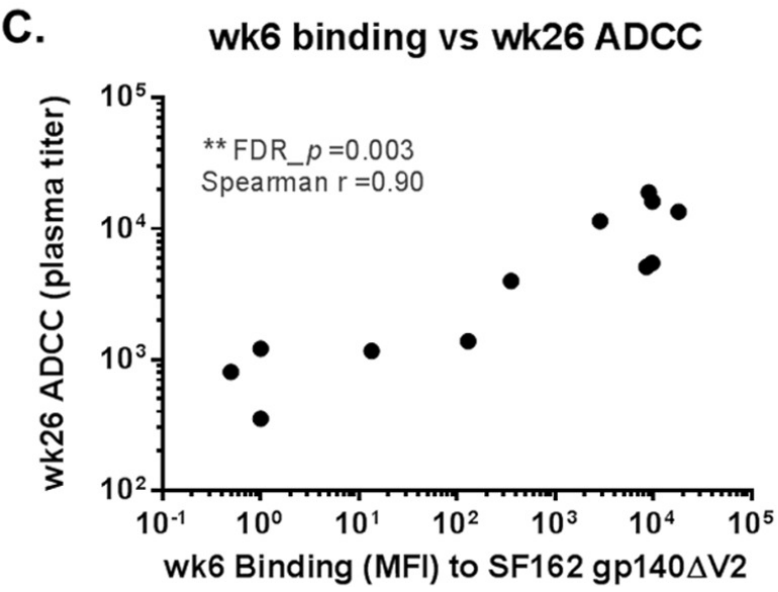
C.
wk6 binding vs wk26 ADCC
** FDR_p =0.003
Spearman r =0.90
wk26 ADCC (plasma titer)
wk6 Binding (MFI) to SF162 gp140ΔV2

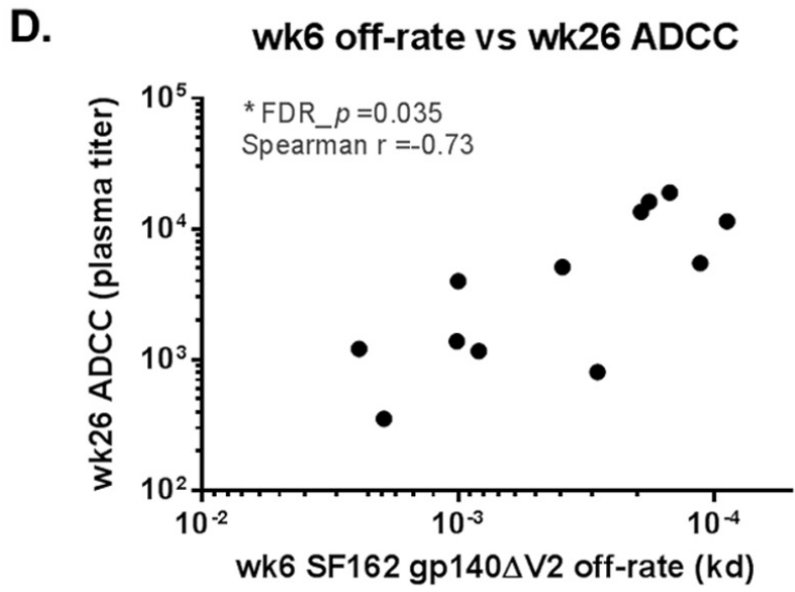
D.
wk6 off-rate vs wk26 ADCC
* FDR_p =0.035
Spearman r =-0.73
wk26 ADCC (plasma titer)
wk6 SF162 gp140ΔV2 off-rate (kd)